SURFACE TENSION OF SOLID COPPER

By

HARRY UDIN

S. B., Massachusetts Institute of Technology, 1937

Submitted in Partial Fulfillment of the

Requirements for the Degree of

DOCTOR OF SCIENCE

from the

Massachusetts Institute of Technology

1949

⟨

Signature of Author
Department of Metallurgy
January 1949

Signature of Professor
in Charge of Research

Signature of Chairman of
Department Committee on
Graduate Students

Foreword

Surface tension is a physical phenomena which is easy to understand, easy to demonstrate qualitatively, but extremely difficult to measure with a high degree of accuracy. Over a period of a century methods have been standardized for measuring the surface tension of water solutions and organic liquids, and these methods have proven quite satisfactory. However, when these same methods are applied to mercury they yield results which vary, from worker to worker, by nearly 100%.

The fault lies more with the material than the method. Mercury has a surface tension some ten-fold that of most non-metallic liquids, and is thus extremely susceptible to surface contamination.

Higher-melting metals, with their higher cohesive energies, have even higher values of surface tension. Thus the problem of developing a technique for measuring the surface tension of metallic solids was approached with due respect for the probable experimental difficulties.

As each possible method presented itself, it was subjected to an exhaustive theoretical investigation. Would it lead to a true value of surface tension? To a less fundamental but equally useful value of interfacial tension under specified conditions? Or to a fictitious value, due to unpredicted and non-reproducible surface contamination? Were the thermodynamic and kinetic premises on which it was based sound ones? If these questions could be answered satisfactorily an estimate was made of the magnitude of the surface tension effect to be measured, and of the technical feasibility of the experiment.

The reader who is interested in this portion of the investigation, which required as much time and considerably more labor than the experi-

mental part, will find it outlined in Section III. The reader who is not interested should at least read pages 26 to 31 as an introduction to the experimental work, Section IV. The handful of previous experiments, and the rather more extensive theoretical work, on the surface tension of solids, are discussed in Section II.

Considerable time and thought was devoted to the design of the experimental equipment. This was time well invested, as only a few days were lost in the whole research due to technical difficulties. Engineering details are given in Appendix F.

Table of Contents

Table of Illustrations

I. Introduction

A. Surface Tension and Metallurgy

Nearly all important chemical and metallurgical reactions either take place at the interface between phases or, if taking place within a phase, result in the formation of a new phase. Even such phenomena as recrystallization and grain growth occur at that elusive interface within a phase which metallurgists call a grain boundary.

It is thus not surprising that physical chemists have devoted a great deal of study to such interfacial parameters as surface tension and adsorption. Metallurgists, on the other hand, were somewhat slower to recognize the importance of surface phenomena in their field. The classic paper of Becker[1] on nucleation in metals aided in breaking down this barrier. Subsequent work on surface phenomena in relation to physical metallurgy has been brought to a focus by C. S. Smith's recent paper, "Grains, Phases, and Interfaces: An Interpretation of Microstructure."[2]

The development of froth flotation brought to one field of metallurgy a keen realization of the importance of surface tension. It was quickly realized that the success or failure of the process depended uniquely on control of the interfacial tension relationships among — at the simplest — four phases, gas, liquid, gangue, and sulfide.

With the growth of powder metallurgy came the realization that the hitherto empirical approach to this field must be replaced by a more scientific approach. It soon became evident that the rate of sintering of powder masses depended to a first degree on the surface

tension of the particles.[3]

In each of these fields, only a qualitative evaluation of the effect of surface energy is feasible, due to the practically complete lack of quantitative data on the surface tension of solids. This thesis consists in part of a critical evaluation of methods of measuring surface energy of solids — including both the few previously proposed in the literature and a number proposed by the author and by his associates — and in part of an experimental determination of the surface tension of solid copper, using the most promising of these methods.

B. General Theory of Surface Tension

Starting with the experimental fact that adsorption exists, Gibbs[4] was able to prove the existence of excess energy at the interface between two phases. His development is fundamental, and is reproduced in abbreviated form below.

Consider a small portion of a system δM, enclosed in an envelope whose only restriction is that it is generated by a straight line L everywhere normal to any surface of discontinuity which it intersects. For the sake of generality, let us define "normal to a surface" as "in the direction of maximum inhomogeneity, with the surface as origin."

Consider two imaginary geometric surfaces PP', parallel to the still indefinite discontinuity, and lying within the homogeneous regions of the two phases. (Figure 1)

Figure 1: SECTION THROUGH A SURFACE

The inhomogenous layer is enclosed within the

dotted lines.
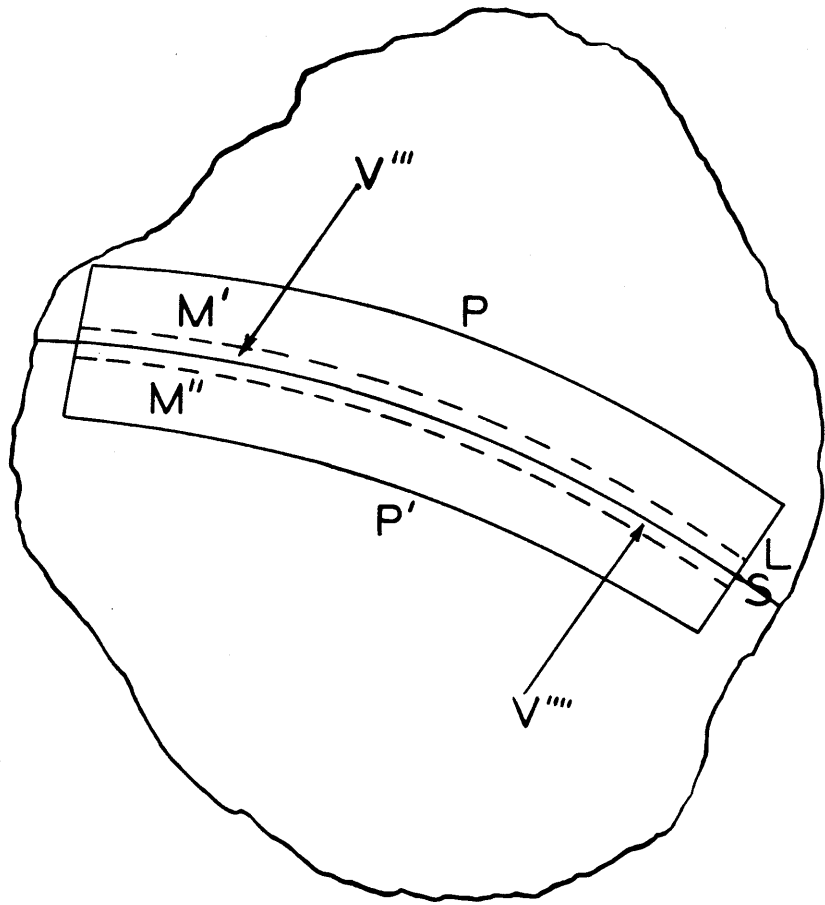
Let δM = mass enclosed by PP' and the envelope

$\delta M'$ = mass of homogeneous A in δM

$\delta M''$ = mass of homogeneous B in δM

For each of these masses we can write:

$$\delta E = T \delta S + \Sigma \mu_i \delta n_i \tag{1}$$

$$\delta E' = T \delta S' + \Sigma \mu_i' \delta n_i' \tag{2}$$

$$\delta E'' = T \delta S'' + \Sigma \mu_i'' \delta n_i'' \tag{3}$$

The symbols have their usual thermodynamic meaning.

Assume for the moment that the surface of discontinuity can be located at S. (Its actual location within the inhomogeneous layer will be shown to be immaterial, within certain limitations.) S divides the inhomogeneous layer into two volumes, $\delta v'^{*}$ adjacent to $\delta M'$, and $\delta v''^{*}$ adjacent to $\delta M''$. Imagine these two volumes to be filled with material having the same properties (T, P, μ etc.) as $\delta M'$ and $\delta M''$ respectively.

Thus, at equilibrium:

$$\delta E'^{*} = T \delta S'^{*} + \Sigma \mu_i' \delta n_i''' \tag{4}$$

$$\delta E''^{*} = T \delta S''^{*} + \Sigma \mu_i'' \delta n_i'''' \tag{5}$$

In making the assumption of homogeneity we have set up an inequality between equation (1) on the one hand, and (2) + (3) + (4) + (5) on the other. This leads to:

$$\delta(E-E'-E''-E'^{*}-E''^{*}) = T \delta(S-S'-S''-S'^{*}-S''^{*})$$
$$+ \Sigma \mu_i \, dn_i - \Sigma \mu_i' \delta(n_i' + n_i''') - \Sigma \mu_i'' \delta(n_i'' + \delta n_i'''') \tag{6}$$

If the inequality is concentrated at S, we obtain

$$\delta E^{S} = T \delta S^{S} + \Sigma \mu_i^{S} \delta n_i^{S} \tag{7}$$

It is now necessary to consider the effect of variations in

s on equation (7). Rotation or translation of s will not effect δE^s, but a change in shape of s will. So we can write:

$$\delta(\delta E^s) = f(\delta s, \delta c_1, \delta c_2) \tag{8}$$

where c_1 and c_2 are principal curvatures of s.

If s is sufficiently small so that its curvature is uniform, we can say:

$$\delta E^s = T \delta S^s + \sum \mu_i^s \delta n_i^s + \gamma \delta s + K_1 \delta c_1 + K_2 \delta c_2 \tag{9}$$

γ, K_1, + K_2 are, for the time being, arbitrary constants.

Consider now the last three terms of equation (9). By simple algebra,

$$K_1 \delta c_1 + K_2 \delta c_2 = 1/2(K_1 + K_2) \delta(c_1 + c_2) + 1/2(K_1 - K_2) \delta(c_1 - c_2) \tag{10}$$

γ is of the same order as δE^s, as it is a function of the change in area due to changing curvature. But, if the radius of curvature greatly exceeds the thickness of v''' + v''', K_1 and K_2 are of the order of $\delta\delta E^s$. Furthermore, Gibbs[5] shows that for any shape of s a position for s can be found such that K_1 + K_2 = 0. Thus of the three terms introduced by considering change of curvature of the interface, only $\gamma \delta s$ is of any significance. However, it is important to note that we can never quite make $1/2(K_1 - K_2) \delta(c_1 - c_2)$ vanish, since the layer of inhomogeneity never reaches differential thickness.

Since none of the above operations have disturbed surfaces P and P', we may write:

$$\delta E = T \delta S + \sum \mu_i' \delta n_i' + \sum \mu_i'' \delta n_i'' + \sum \mu_i^s \delta n_i^s + \gamma \delta s \tag{11}$$

However:

$$\delta E = \delta F - \left[P \delta V + V \delta P - T \delta S - S \delta T + O(\delta\delta E) \right] \tag{12}$$

where the last term is of the order of a second differential and may be neglected. Making this substitution and differentiating at constant P, V, T, μ_i yields:

$$\frac{\partial \delta F}{\partial s} = \gamma \qquad (13)$$

Note that s is a macroscopically small surface area and δF is the free energy of the macroscopically small volume enclosed by PLP'L and including s. Let us define F as $\Sigma \delta F$, where the summation is taken over all surface zones where the restrictions in the above development apply. This yields the usual defining expression for surface tension:

$$\frac{\partial F}{\partial s} = \gamma \qquad (14)$$

Note, however, that in the summation we carefully avoid any zones whose radii of curvature are of the same order as the thickness of the adsorbed layer. In a reasonably-sized phase such areas can have only a negligible effect on γ. They are probably important to colloidal phenomena and certain types of catalysis. The author believes that they should also be considered in any theoretical analysis of nucleation.

II. The Surface Tension of Solids

A. Basic Concepts

Since any consideration of the surface adds a degree of freedom to the thermodynamic system, all parameters will be affected by the geometry of the system. Let us consider a spherical surface in equilibrium with its vapor at pressure p, and a plane surface of the same substance at a vapor pressure of p_0. It is shown below that p_0 is less than p, and the difference is a function of the surface tension of the substance: i.e., its interfacial energy in contact with its own vapor only.

(1) Transfer dn mols from the plane to the spherical body.

$$dF = dnRT \ln \frac{p}{p_0}$$

(2) This process increases the volume of the sphere, and therefore its area, without changing the area of the plane, and without altering any of the other thermo-dynamic properties of the system: that is

$$dF = \gamma ds$$

Equating (1) and (2) yields

$$dnRT \ln \frac{p}{p_0} = \gamma ds \qquad (3)$$

If the sphere has radius r, molar volume V, and contains n mols:

$$nV = 4/3 \pi r^3 \qquad (4)$$

$$dn = \frac{4 \pi r^2}{V} dr \qquad (5)$$

Further: $\qquad ds = 8 \pi r dr \qquad (6)$

Substituting (5) and (6) into (3) yields:

$$RT \ln \frac{p}{p_0} = \frac{2\gamma V}{r} = \frac{2\gamma M}{\rho r} \tag{7}$$

where M is the molecular weight and ρ is the density of the phase. This is the well-known Kelvin equation.

The concept of surface tension in a solid is a difficult one. To the thermodynamicist a solid is a solid, and can respond to a force only by mass motion without distortion. Saal and Blott[6] go so far as to question the validity of the Kelvin equation as applied to a solid phase, since it is derived for a fluid sphere. Nevertheless, most of the few experimental observations of surface tension of solids have been based on thermodynamic properties; and of these some are based on the Kelvin equation.

W. Ostwald in 1900 observed that very finely divided mercurous oxide suspended in aqueous salt solutions coarsened quite rapidly[7]. Pawlow[8] actually observed under the microscope the growth of fine crystals at the expense of finer ones, by vapor phase transport. He worked with a series of easily volatilized organic solids such as biphenyl-methane and iodoform. The kinetics of the process is far too complicated to permit a quantitative evaluation of surface tension, but the observations disprove the reasoning of Kossel[9] and of Saal and Blott, that is, that there could be no size effect on the vapor pressure of solids, since a given crystal face has a given vapor pressure, regardless of its area.

Hüttig[10] and co-workers measured the total surface area of a sample of copper powder by carefully conducted adsorption isotherm determinations. They also measured the electromotive force of the powder against massive copper in a buffered copper sulfate electrolyte. In a derivation completely analagous to that leading to equation (7), page 7, it can be shown that

$$\gamma = \frac{\mathcal{F} V r \rho}{2 M} \qquad (8)$$

where $\mathcal{F}$ = Faraday's constant

V = EMF of cell

r = radius of particles

Application of equation (8) to Hüttig's data yields a value of about 40,000 ergs-centimeter^{-2}, some 30 times too high.

On the other hand, Fricke and Meyer[11] obtained a value for gold of 670 ergs-centimeter^{-2}, a value probably about 50% too low. They made a gold sol by reduction of a solution of a gold salt. Average particle size was estimated by measuring the broadening of X-ray diffraction lines, and total surface was calculated on the assumption of cubical particles. Surface energy was determined calorimetrically, by measuring the heat of solution of the powder in iodine trichloride. The heat of solution of massive gold is used as a reference zero. The method of obtaining ΔF^S from ΔH^S will be discussed later in this chapter.

These two experiments exhaust the reported work on the thermodynamic determination of the surface tension of metallic solids. Even less work has been done on solid non-metals. Lipsett, Johnson,

and Mass[12] made a sodium chloride sublimate which they classified by air elutriation. The heat of solution of a uniformly sized fraction of the powder was compared to the value for massive crystals. Particle size was determined microscopically. The value of total surface energy, ΔH^S, was found to be 356-406 erg-centimeter^{-2}, with large variations from test to test.

The experiments discussed to this point have all been based either on the Kelvin equation or on a direct measurement of surface energy. The surface effect is, however, much more general than indicated by this discussion. When the surfaces and interfaces of a thermodynamic system are considered as part of the system, it is evident that we have introduced a new degree of freedom, namely, the geometry of the system.

Meissner[13] shows that fine lamellae will have a lower melting point than massive crystals of the same composition, and relates the depression of the melting point to the (Helmholtz) free energy of the surface by the following expression for lamellar-shaped particles:

$$\Delta A_0 = \frac{T_0 - T}{T_0} \Delta H_f \frac{\rho\, d}{2}$$

ΔA_0 = (Helmholtz) free energy per unit area of surface

T_0 = melting point of massive crystals

T = melting point of fine crystals

d = thickness of fine crystals

ρ = density

ΔH_f = heat of fusion

His experiments led to reasonable values for organic solids. Skapski[14] proposes to apply this method to sheets of metal foil sandwiched between optical flats of quartz. Some old work of Turner[15], discussed later in this chapter, indicates that the experimental difficulties will be formidable.

B. Viewpoint of Harkins, Frenkel and Others

According to Harkins, a knowledge of the surface tension of solids is fundamental to the understanding of many physico-chemical phenomena. In the absence of reliable experimental methods, he has attempted an approximate calculation of surface energy on simple theoretical grounds.[16] His premises are as follows:

1. Surface tension owes its existence to the presence of unsatisfied chemical bonds—ionic, covalent, metallic, or Van der Waal's, as the case may be—at the surface of the phase.

2. For a crystalline solid the number of these bonds can be calculated for any crystallographic face. The face of lowest energy will be a plane of densest packing (fewest broken bonds).

3. The total heat content (ΔH) of a mol of bonds can be calculated from the heat of vaporization of the solid.

4. For the free energy of a mol of bonds:

    a. assume ΔH^S is independent of temperature

    b. assume that $\Delta F^S = \Delta H^S$ at $T = 0$, that
$\Delta F^S = 0$ at the critical temperature where liquid and gas are indistinguishable, and it is a linear function of temperature. This is essentially a

thermodynamic expression for the empirical Eötvös

equation $C \gamma = K(T_c - T)$, where C is a function of

the atomic volume.

5. The decrease in surface energy due to distortion of the

atomic bonds in the surface layer is neglected.

Harkins performs his calculation on diamond, and obtains, at

room temperature, free energies of 5400 ergs-centimeter^{-2} for a (111)

face and 9400 ergs-centimeter^{-2} for a (100) face. A similar calcula-

tion for a (111) face of copper has been made by the author.

A copper atom has 12 nearest neighbor bonds. Cleaving the

lattice parallel to a 111 array of atoms fractures three of these

bonds (Figure 2). The heat of vaporization of copper is given by

Kelley[17] as 70,300 calories per mol of atoms, equivalent to 5860

calories per mol of bonds.

The interatomic spacing in copper is 2.551 Å,[18] so a 60°

parallelogram one centimeter on a side will contain $10^{16}/(2.551)^2$

atoms and will have an area of $\sqrt{3}/2$ centimeters^2. The surface

density is thus $\dfrac{2 \times 10^{16}}{\sqrt{3} \times (2.551)^2}$ atoms per centimeter^2, or

$$\dfrac{2\sqrt{3} \times 10^{16}}{(2.551)^2} \quad \text{free bonds per centimeter}^2$$

The surface total energy is thus

$$\dfrac{5860 \times 2\sqrt{3} \times 10^{16}}{(2.551)^2 \times 6.02 \times 10^{23}} \times 4.186 \times 10^7 = 2170 \text{ ergs/cm}^2$$

$$\dfrac{cal}{mol} \times \dfrac{bonds}{cm^2} \times \dfrac{(bonds)^{-1}}{(mol\ )} \times \dfrac{ergs}{cal} = \text{ergs/cm}^2$$

Figure 2: A (III) PLANE IN THE CUBIC CLOSE-PACKED SYSTEM

The central atom and six of its neighbors are in
the surface. Three nearest neighbors lie below
the surface. Three more, shown dotted, are
removed by cleavage.
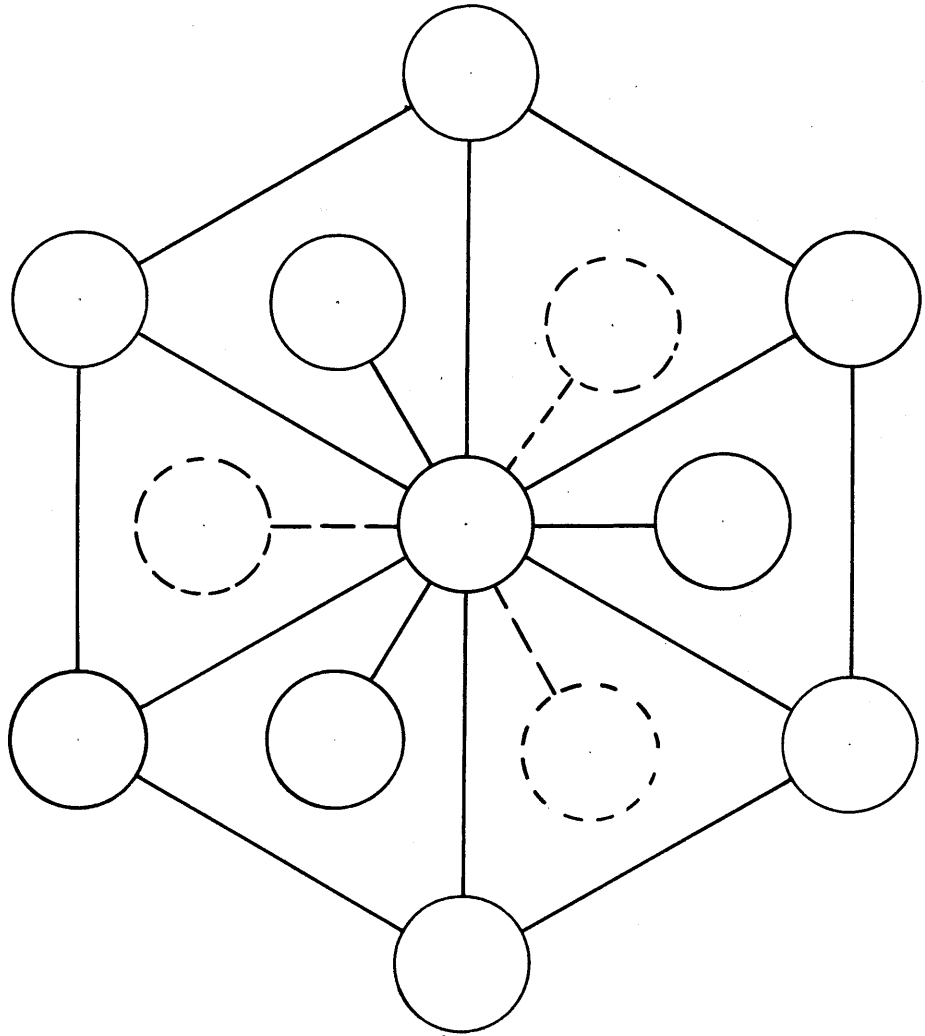
If the boiling point of copper is taken as 0.63 times the critical temperature[16] the indicated point of zero surface tension is 4100°K, with a large uncertainty. The surface tension may then be expressed as:

$$\gamma = 2170 - 0.53 \ T$$

Frenkel[19] showed that the interfacial tension between pure solid and liquid at the melting point is of the order of 1 dyne per centimeter, and therefore the surface tension of a pure material in its solid state must closely approximate the more easily measured surface tension in the liquid state. (Antonow's rule[6] states that $\gamma_{12} = | \gamma_1' - \gamma_2' |$, where γ_{12} is the interfacial tension between two phases; γ_1' is the surface tension of phase 1; and γ_2' is the surface tension of phase 2, when the two phases are mutually saturated.)

Turnbull[20], on the other hand, finds that the interfacial tension between liquid and solid gallium is of the order of 100 ergs-centimeter^2. Both may be right. In cases where both liquid and solid have close-packed structures, the interfacial tension may be very small, whereas in cases where the liquid has a closer packing than the solid, the tension may be higher. Frenkel pointed out that as the melting or freezing point is approached, the material shows a deviation from its normal specific heat in the direction of the specific heat of the future state. If the deviation is assumed to be entirely a contribution of the embryonic future phase, the concentration of embryonic material can be calculated as a function of temperature. The size distribution function at any assumed concen-

tration can be calculated by the kinetic theory of condensed phases. Thus the total interfacial area between parent and embryo phases is established, as is the number of embryonic particles.

The stable phase tolerates these embryos because of their contribution to the entropy of the system[21], which can be calculated. Nevertheless, the individual embryos are unstable with respect to both surface and volume energy. At equilibrium, $\Delta F = 0$, and

$$T\Delta S = \gamma_{12}s + n\Delta F_f$$

To recapitulate:

ΔS is the entropy of mixing of solid embryos and liquid atoms.

γ is the interfacial tension between solid and liquid.

s is the surface area of solid embryos.

n is the mol fraction of embryonic material.

ΔF_f is the free energy of fusion at T.

Of these terms only γ_{12} is unknown. The same equation can be applied to melting.

Frenkel shows that if $\gamma_{12} \approx 1$, as is indicated from the behavior of C_p, then the maximum nucleation rate in freezing should occur approximately 1% below the freezing point. This appears to be in agreement with experiment.

The experimental work on the surface tension of solids is too scanty to serve as a basis for the formulation of a general theory. The theoretical work, though quite voluminous, does not lead to any conclusions amenable to experimental confirmation.

J. Frenkel[22] showed in 1917 that $\gamma = 1/8\pi \int_{-\infty}^{\infty} E^2 \, dx$ where

E is the diffuse–double layer potential. Thus theoretical deter-
minations of y by physicists have generally consisted of attempts
at evaluation of E (x), at first by classical and later by quantum-
mechanical calculations.

Dorfman[23] showed that:

$$y = \frac{8.7 \times 10^{10} \, (Z_i)^{1/2} \, (\chi_{j_i})^{3/2}}{A^2} + 4.22 \, (\phi_o)^{9/4}$$

where Z_i = number of free electrons per ion

χ_{j_i} = diamagnetic susceptibility

A = atomic volume

ϕ_o = a function of Fermi distribution of the surface electrons.
Calculations of the surface energy of metals based on this equation
give results of the correct order of magnitude.

Brager and Schuchowitzky[24] calculated the total energy E_N
of the free electrons of a finite piece of metal. They used the
Sommerfeld model of a monovalent metal, and made the calculation
for one octant of a sphere. The resulting expression is:

$$E_N = \alpha \left[\frac{\pi b^5}{5} N^3 + \frac{3\pi b^4}{8} N^2 + O(N^{1.4}) \right]$$

where $\alpha = \dfrac{h^2}{8 \, m\Delta^2}$

$b = \sqrt[3]{3/\pi}$

Δ = lattice constant

N^3 = number of lattice sites in piece of metal considered.
In this expression, the first term is the Fermi energy of the
electrons within the metal, and the second that of the surface
electrons. The third term, a function of the geometry of the

specimen, is of the order of $N^{1.4}$ and may thus be neglected. From the second term it follows that

$$\gamma = \frac{h^2 \pi b^4}{128m} \left(\frac{\rho}{M}\right)^{4/3}$$

where ρ and M are the density and atomic weight of the metal. The universal constants of the coefficient evaluate to 56,400 if $m = m_e$. If the periodicity of the positive field within the metal and at its surface is considered by taking the effective mass of an electron in a metal as 2-2.5 m_e, the calculated surface tensions are in fair general agreement with experimental values.

However, the authors state that if the few experimental values for the surface tension of liquid metals are plotted in the form "log γ against log $\frac{\rho}{M}$", the slope is about 1.2, not 1.33. The experimental values are so fragmentary and uncertain that the discrepancy is not significant.

C. Experimental Observations of the Mechanical Effect of Surface Tension

Over the past seventy-five years there have been sporadic observations of surface tension effects in gold leaf.

Turner[25] noted that when gold-beaters' leaf is heated to 550° between glass flats, it shrinks and becomes transparent. He found the same effect with heated silver and copper foils. Both the shrinkage and the micro-tearing were attributed to the effect of surface tension.

Chapman and Porter[26] decided that the micro-tearing was caused by the constraining effect of the glass flats. They cemented

gold leaf to a loop of platinum wire. When this specimen was heated, it developed large tears, again due to the surface tension forces. Accordingly, they made specimens of the form illustrated in Figure 3a. They found that "rapid" contraction of this specimen commenced at $340^{\circ}C$, for loads of 6.6 to 26.7 milligrams. For 0.001 inch gold wire and a load of "the minimum weight required to keep the wire taut" the wire invariably stretched when heated.

Sawai and Nishida[27] attempted quantitative measurements on a similar configuration of specimen. (Figure 3b) They tested beaten gold leaf 0.77 microns thick and beaten silver leaf 0.63 microns thick, of which they say merely "the specimens showed no preferred orientation". The change in length of the specimens was plotted against load. Surface tension was calculated from the load which resulted in no change of length according to the relationship

$$\gamma = \frac{P}{2W}$$

when P = load and W = specimen width. A critical discussion of this relationship is presented in the next section of this thesis.

Results were very erratic, but were in general lower than published values for the corresponding molten metal. An anomalous decrease in γ with decreasing temperature was noted.

Tammann and Boehme[28] repeated this work, using electrolytically deposited gold lamellae. They objected to the use of beaten leaf because of its non-uniformity in thickness. They eliminated time as a variable by plotting $\frac{\Delta \ell}{\ell t}$ against load and got reasonably consistent values. From experiments at 700°, 750°, 800°, and 850°

Figure 3a: CHAPMAN FOIL SPECIMEN

Figure 3b: SAWAI AND NISHIDI FOIL SPECIMEN

The weights are cemented on.   Dimensions are

in cm.

1

1½

WGT.

½
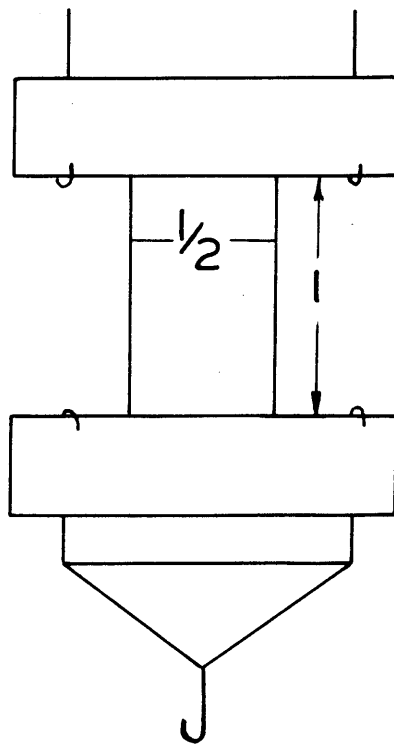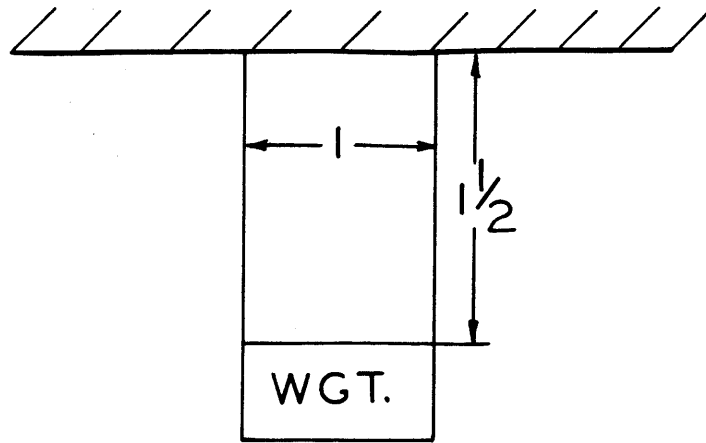
they concluded, for gold, that $\gamma = 1200$ milligrams per centimeter at $800^{\circ}C$, and $\frac{d\gamma}{dT} = -0.4$ to -0.33 milligrams per centimeter $^{\circ}C$.

III. Evaluation of Experimental Methods for Metals

The experimental methods discussed in this section were investigated exhaustively only if it appeared that they were experimentally feasible and would lead to a value for surface tension without any serious approximations and with no unjustifiable assumptions. Thermodynamic as well as mechanical manifestations of surface energy were considered. All analyses were made on the assumption that copper would be the metal tested, except where good reasons existed for considering another metal. From an experimental standpoint, copper, silver and gold appear as the simplest materials to operate with.

A. Thermodynamic Measurements

1. Selective Distillation of Powder Particles

The effect of surface energy on thermodynamic properties was shown by Kelvin to be a function of the radius of curvature of the surface. Thus the vapor pressure of small particles of radius "r" is expressed by:

$$\ln p_r/p_\infty = 2 \gamma M/\rho \, RT \cdot 1/r \qquad (1)$$

where M is the molecular weight of the vapor phase and ρ is the density of the solid phase. Well-authenticated data for p_∞ as a function of T can be found in the literature.[17]

If small metal particles are distilled isothermally in vacuo towards a plane surface of the same metal, at a distance nearer than the mean free path in the metal vapor, the rate of transfer is expressed, according to kinetic theory[29], by:

$$G = 22.15 \sqrt{M/T} \, (p_\infty - p_r) \qquad (2)$$

where "p" is the vapor pressure in atmospheres, and "g" is the rate of transfer of metal, in grams per second per centimeter^{-2} of the smaller surface. Evidently, as it is impracticable to measure the effective area of the powder, this area must be kept larger than that of the plane metallic surface.

Equation (1) may be expressed in exponential form. Furthermore,

$$p_\infty = \exp \left(-\Delta F_T^o / RT \right) \qquad (3)$$

Combining these with equation (2) gives:

$$G = 22.15 \sqrt{M/T} \, e^{\frac{-\Delta F^o}{RT}} \left(e^{\frac{2\gamma M.1}{\rho RT \, r}} - 1 \right)$$

As the pressure difference is extremely small, the exponential within the parentheses is very nearly equal to one plus the exponent. Evaluating the constants gives:

$$G = (0.0364/rT^{3/2}) e^{-\Delta F^o / RT} \qquad (4)$$

where γ for copper is here assumed tentatively to be 1200 erg-centimeter^{-2}, the most probable value in the literature. From Kelley's expression for the free energy of sublimation of copper:

$$\Delta F^o / RT = 41132/T + .237 \ln T + .000368 \, T - 17.82 \quad .$$

If the receiver is a disc of copper, 5 centimeters^2 in area by .02 centimeter thick, it will weigh about one gram, and its weight change can be determined to $\pm$ 10 micro-grams. Thus a total transfer of one milligram of copper will give a weight accuracy of 1 percent. A reasonable time for the experiment would be $5 \cdot 10^5$ seconds, about six days, so a value of G of the order of $4 \cdot 10^{-10}$

would be desirable. By substituting T = 1200°K into equation (4), it can be shown that powder as coarse as 10 microns can be used.

As previously mentioned, the effective area of exposed powder must be greater than that of the target. Furthermore, it must be sufficiently great so that loss of 1 milligram of copper will not decrease the particle radius significantly. A 5 percent decrease in radius would entail a 2.5 percent error in γ, which is tolerable. With this criterion, the minimum weight of exposed powder can be calculated, as:

$$w_o = \Delta w r_o^3 / (r_o^3 - r_f^3)$$

For r_o = 0.95 r_f, w_o calculates to be 0.007 gram. As 0.007 gram of powder with radius of 10^{-4} centimeters would have a surface of 23 centimeters^2, some ten milligrams of exposed powder is sufficient for the experiment.

The problem of exposing sufficient powder to the proper evaporating conditions is a difficult one. To avoid sintering, it will be necessary to disperse the powder in some medium such as superfine graphite. If this is overcome, the method appears feasible.

2. Selective Distillation of Wires

A similar experiment might be run, using a fine wire suspended in a copper tube. In this case, the effective area is that of the wire, and the amount of copper transferred could be determined most accurately by measuring the decrease in diameter of the wire. The same equations apply, except that for a cylinder subliming isothermally towards a plane, (see Appendix A)

$$\ln p_r/p_\infty = (\gamma M/\rho RT) (1/r)$$

so that wire of diameter "d" is equivalent to powder of radius "r" when d = r.

Of course the approximation of constant diameter can no longer hold. However, $G(p)$ and $p(r)$ are known, so an expression of t in terms of r can be calculated. For a cylinder:

$$G = - \rho dr/dt, \qquad so:$$

$$-dr/dt = B(p - p_\infty), \quad \text{where } B = (22.15/\rho) \sqrt{M/T} \qquad (1)$$

$$p = p_\infty e^{A/r}, \qquad \text{where } A = 2\gamma M/\rho RT \qquad (2)$$

Substituting (2) into (1) gives:

$$- \frac{1}{B} \frac{dr}{dt} = p_\infty (e^{A/r} - 1) \qquad (3)$$

As in the previous derivation, $e^{A/r} - 1$ is very nearly equal to A/r, for small values of the exponent. Making this substitution gives:

$$-rdr = p_\infty AB \, dt \qquad (4)$$

$$t = \frac{r_o^2 - r_f^2}{2p_\infty AB} \qquad (5)$$

For an initial diameter (effective radius) of 0.0025 centimeter, and a final radius of 0.001, (finer wires could not be measured with sufficient accuracy) and a temperature of 1050°C, "t" evaluates to $6 \cdot 10^{10}$ seconds, which is excessive by a factor of 10^5.

If the wire were allowed to evaporate toward a surface in which the activity of copper approximated zero at low concentrations,

as a nickel shield, this time could be reduced by a factor of 10^6. It would be impossible to control the temperature so closely as to distinguish between p_r and p_∞, even if ΔF^0 of sublimation were known with sufficient accuracy. However, an experiment can be conceived whereby two wires of different diameters would be evaporated at the same time. The difference in decrease of radii would be a measure of p_r/p_∞. A simple numerical calculation shows that this is impractical. For a diameter of 0.001 centimeter, p_r is approximately equal to 1.0001 p_∞. Thus the smaller radius would decrease only .01 percent faster than the larger. For an accuracy of $\pm$ 10 percent in γ it would be necessary to measure the wires to 0.001 percent or $\pm 10^{-8}$ centimeters.

It is unfortunate that distillation of a copper wire toward a copper cylinder is too slow, as it is otherwise a nice technique. Possibly, it would be applicable to the determination of surface tension of magnesium, as the latter metal has a considerably higher vapor pressure near its melting point. Other metals to which either the powder or wire techniques might apply are listed in the Appendix.

3. Other Thermodynamic Experiments

A surface energy effect other than vapor pressure might be used as a parameter. Solubility and electromotive force are possibilities.

If dn mol of copper is transferred electrolytically from a plane surface to the surface of particles of radius "r", the free energy change would be:

$$d \Delta F = RT \ln \left(\pi_r / \pi_\infty \right) dn$$

where π is the solution pressure of copper against the electrolyte. $\mathcal{E}$, the electromotive force, equals $RT/z\mathcal{F} \ln \pi_r/\pi_\infty$, so

$$d \Delta F = \mathcal{E} z \mathcal{F} dn = \gamma ds$$

If a particle containing n mol has a radius r, then:

$$nM/\rho = (4/3) \pi r^3$$
$$dn = (4 \pi r^2 \rho/M)dr$$
$$s = 4 \pi r^2$$
$$ds = 8 \pi r dr$$

so,

$$\mathcal{E} = (\gamma/z\mathcal{F}) (ds/dn) = 2 \gamma M/\mathcal{F} r \rho$$

For one micron powder, which could be prepared without too much difficulty, in a uniform particle size and shape, the electromotive force would be 174 microvolts, which could readily be measured to ± 2 percent.

The value of γ thus obtained would be the interfacial tension of copper against the electrolyte. To obtain the true surface tension of copper the free energy of emersion of copper from the electrolyte would be required. Free energies of emersion of metal powders from inert liquids can be calculated from the heat of wetting, determined by methods of precision calorimetry.[30] For clean metals in n-heptane, they are of the order of magnitude of 500 ergs per square centimeter, equivalent to about 0.5 calories per gram of 0.2 micron powder. However, in this case, where chemical side reactions would be difficult to suppress, as between copper and dissolved oxygen,

the calorimetric determination appears impractical.

For a system of solid, liquid, and gas in mutual contact[31]

$$\gamma_{SG} = \gamma_{LG} \cos\alpha + \gamma_{LS}$$

α, the contact angle between electrolyte and copper, is zero. The electromotive force measurement would give γ_{LS}, and values of γ_{LG} can be found in the literature, if a copper sulfate electrolyte is used. The sum, γ_{SG}, is the surface energy of copper saturated with adsorbed water vapor. Neither γ_{LS} nor γ_{SG} can be used as even a qualitative indication of γ_{Cu}. The justification for this statement lies in the extreme tenacity with which a solid surface retains its last monolayer of adsorbed water during outgassing. Such an experiment would, however, be valuable in supplying contributory information on the surface energy of copper.

The solubility of fine copper powder in a molten metal, or conversely, of a molten metal in fine copper, could possibly be measured and compared with the solubility of or in massive copper at the same temperature. Aside from the experimental difficulties, this is also open to the objection that only an interfacial tension would be obtained, as in the electrolytic case. A summary of possible binary systems to which this method can apply is given in the Appendix.

The surface energy of copper could be determined approximately by a method analagous to that used for sodium chloride.[12] The heat of solution of finely divided copper in mercury can be determined calorimetrically and compared to that of coarse copper. The difference represents the total surface energy of the powder. From this the surface free energy could be calculated by making the

assumptions listed on page 10 . The experiment would be a valuable
one. It is safe to assume that the latent energy is a relatively
small part of the total surface energy, and the errors introduced by
the assumptions would be proportionately small.

Decrease in melting point of finely divided metal can also be
used as a measure of surface tension. One worker[14] proposes to
flatten a droplet of metal between two optical flats of quartz and
determine its melting point by observing the discontinuity in its
optical reflectivity upon melting. The relationship between surface
energy, thickness, and lowering of melting point has already been
discussed. The problems of making and maintaining a uniform thick-
ness of the lamellae, and of avoiding the micro-tearing described
by Turner appear extremely difficult. Also, since the method leads
to the interfacial tension of the metal against quartz, no quantitative
evaluation of its feasibility has been made.

B. Mechanical Measurements

1. The Sawai - Tammann Technique

In the familiar soap-film demonstration of surface tension
a film is stretched over a wire frame with one movable side, and
the tension on the movable side is measured. For this case $\gamma = P/2W$.
At first glance, the Sawai - Nishidi specimen is completely anala-
gous to this. However, careful consideration shows that in the
soap-film, the transverse forces are balanced by the fixed sides of
the wire frame, whereas unbalanced forces exist in the transverse
direction in the metal foil. The stresses and resultant strains
cannot be handled analytically for these particular boundary conditions,

but it is sufficient to state qualitatively that if the tendency
of the strip to become "wasp-waisted" is of the same order of magni-
tude as the tendency of the strip to shrink longitudinally, the net
load for zero longitudinal strain will be considerably less than
$2\gamma W$. Thermodynamically, we can visualize the surface area decreasing
by a thickening of the specimen while its length remains constant.
Because of this uncertainty, the use of foil for measuring the sur-
face tension of solid metal was not considered.

2. Strains in Wires

In contrast to a specimen of thin foil, the strains in a
fine wire can be handled mathematically. Consider a series of small
weights of increasing magnitude suspended from a group of fine copper
wires of uniform length and diameter, and the system brought to a
temperature at which creep is appreciable under vanishingly small
stresses. If the weight overbalances the contracting force of
surface tension the wire stretches; otherwise it shrinks. The
magnitude of the strain is determined by the amount of unbalance,
so a plot of strain versus load should cross the zero strain axis
at $w = F_\gamma$, where F_γ is the longitudinal stress due to surface ten-
sion. If balance is visualized as a thermodynamic equilibrium, the
critical load is readily calculated. An infinitesimal change in
surface energy must be equal to the work done on or by the weight:

$$\gamma ds = wdl \qquad (1)$$

For a cylinder of radius r and length l,

$$s = 2\pi r^2 + 2\pi rl \qquad (2)$$

Since the volume remains constant,

$$r = \sqrt{V/\pi l} \tag{3}$$

$$s = 2\sqrt{\pi V l} + 2V/l \tag{4}$$

$$ds = (\sqrt{\pi V}/l - 2V/l^2)\, dl \tag{5}$$

Substituting (5) into (1) gives for the equilibrium load,

$$w = \gamma(\sqrt{\pi V}/l - 2V/l^2) \tag{6}$$

and, again expressing V in terms of r and l,

$$w = \pi r \gamma (1 - 2r/l) \tag{7}$$

The end effect term, $2r/l$, can be neglected for thin wires.

Equation (7) can be confirmed by means of a stress analysis. If the x-axis is chosen along the wire:

$$X_x = \frac{2\pi r \gamma - w}{\pi r^2} \tag{8}$$

As mentioned above, a cylinder of diameter d is equivalent to a sphere of radius r, insofar as radial surface tension effects are concerned, so, neglecting end corrections:

$$Y_y = 2\gamma/d = \gamma/r = Z_z \tag{9}$$

For the case of zero strain in the x direction, the strain must also be zero in the y and z directions. The condition of hydrostatic stressing exists, and (8) may be equated to (9). This yields:

$$2\pi r \gamma - w = \pi r \gamma \tag{10}$$

$$w = \pi r \gamma \tag{11}$$

The end correction term was dropped implicitly in equation (9), which is written for an infinite cylinder.

One mil copper wire is readily obtained commercially. For this diameter, $w = 4.8$ dynes, or 4.8 milligrams nearly; it is

anticipated that a range of loads from 1/2 w to 2 w would be used.

Three criteria for a successful experiment have been considered. There are undoubtedly others.

(1) Accurately measurable strains should be obtained, but the experiment should not be continued to the point where appreciable necking (in the case of extension) or bulging (in the case of contraction) occurs.

(2) In order that the mode of strain be the same for each specimen, the critical shear stress for slip should not be exceeded at maximum effective load.

(3) The wire weight should be negligible compared to the minimum load, so that no significant variation of stress exists along the wire.

For one mil wire the wire weight is 0.045 milligram per centimeter, or about 2 percent of the minimum load. However, at 5 milligram maximum effective load, the tensile stress is 1000 grams per centimeter^2, or 15 psi, which may be beyond the microcreep range near the melting point.

For five mil wire the range of loads would be 12 to 48 milligrams. The wire weight is 1.1 milligrams per centimeter. While this weight is not negligible compared to 12 milligrams, the error introduced by considering one half of it to be concentrated at each end of the wire is less than the probable experimental error. The tensile stress at 48 milligram load is only 2.6 psi. Three mil wire might be a better compromise than five mil.

With certain assumptions, it is possible to calculate the strain rate. If pure viscous flow is assumed, there will be no change in lattice energy, and all the strain energy will appear as heat. If the kinetic energy of the moving weight is neglected, the time rate of heat generation must be equal to the rate of change of potential energy of the system. The system changes its energy by changing both the level of the weight and the amount of copper surface. Thus:

$$dQ/dt = wdl/dt - \gamma ds/dt \tag{12}$$

Frenkel[32] showed that for a viscous rod being extended longitudinally,

$$dQ/dt = (6\eta V/l^2)(dl/dt)^2 \tag{13}$$

where η is the coefficient of viscosity. From equation (5):

$$ds/dt = (\sqrt{\pi V}/l - 2V/l^2)dl/dt \tag{14}$$

Dropping the end effect term and combining gives:

$$dl/dt = wl^2/6\eta V - (\gamma/6\eta)\sqrt{\pi/V} (l^{3/2}) \tag{15}$$

This expression is also derived in the appendix by adapting Hooke's Law to viscous flow.[33] The equation can be integrated between $t = 0$ at $\ell = \ell_0$ and $t = t$, $\ell = \ell$. (See Appendix B)

$$t = 12 \eta/\gamma \left(-\Delta r + \frac{w}{\pi\gamma} \ln\left| \frac{\sqrt{l_0}(w\sqrt{l} - \gamma\sqrt{\pi V})}{l\ w\sqrt{l_0} - \gamma\sqrt{\pi V}} \right| \right) \tag{16}$$

From equation (16) the feasibility of the method can be established, at least so far as a reasonable duration of the experiment is concerned. In Figure 4 is plotted the time for 30 percent extension or concentration of three mil wire as a

Figure 4:   THE TIME REQUIRED FOR A FIXED AMOUNT OF STRAIN,

AS A FUNCTION OF LOAD AND TEMPERATURE
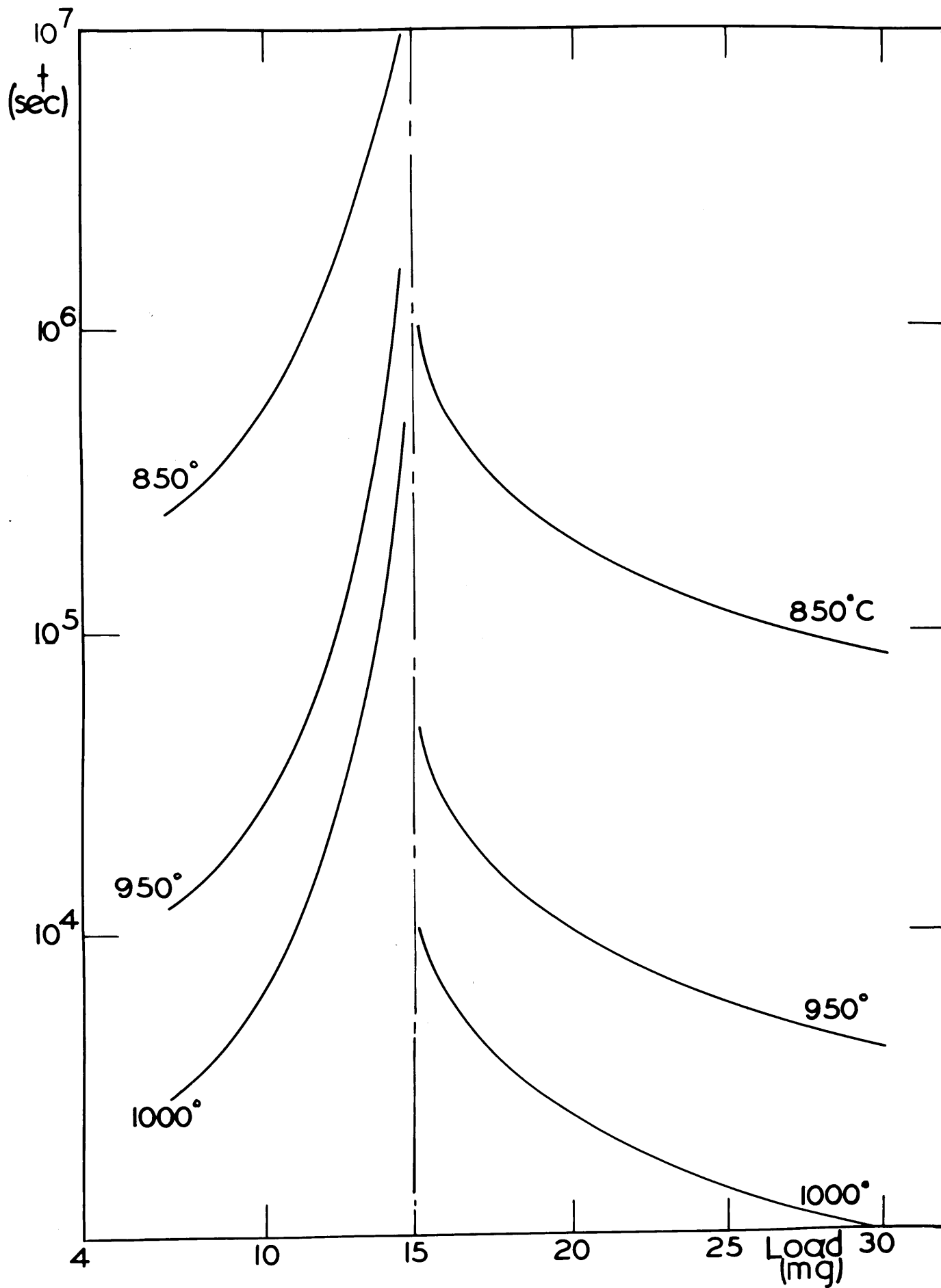
function of load, for several temperatures. η was taken as

$$kT/D \delta \qquad (17)$$

where δ is the nearest neighbor distance and D is the self-diffusion coefficient. Shaler and Wulff[34] determined on the basis of sintering rates that, in the equation

$$D = D_0 \exp(-Q/RT) \qquad (18)$$

the value of Q is 73,000 ± 7000. Figure 4 was plotted on the basis of $D_0 = 1$ and $Q = 80,000$. It can be seen that, despite the large uncertainty in both γ and η, a temperature can be determined experimentally at which strains will be appreciable in a reasonable time.

Ideally, the system should be kept under continuous observation, and the strain of each wire plotted against time. From equation (14), it can be shown that this curve is asymptotic to $t = t_\infty$ at $\ell = \infty$, where t_∞ is a finite time, different for each load. The point at which there occurs a significant deviation from the theoretical curve will indicate where criteria (1) or (2) are exceeded. If continuous observation is not feasible, the accuracy of the method will depend on the magnitude of the strains for loads near balance, for a time within the limit established by criterion (1). This has been calculated from equation (16), assuming that a strain of 75 percent under a 30 milligram load is permissible. For $\ell_0 = 1$ centimeter,

$\Delta \ell = -.011$ cm at 14 mg; $\Delta w = -0.4$ mg

$\Delta \ell = .017$ cm at 15 mg; $\Delta w = 0.6$ mg

$\Delta \ell = 0$ at 14.4 mg; $\Delta w = 0$

where Δ w is the amount of unbalance.

The weight can readily be measured to ± 0.01 milligram. If index marks can be made on the wire its strain can be determined optically to ± 0.001 centimeter. The error in y is proportional to the sum of the error in the weight determination and the error introduced by the uncertainty in Δl. For the example calculated, ± 0.001 centimeter introduces an uncertainty of 0.04 milligram in Δ w, so the accuracy would be ± 0.3 percent. There is ample margin for overoptimistic estimates of precision of measurements and permissible strain.

3. Strains in Thin Discs

Equation (7), page 27, is perfectly general for cylindrical shapes, and can be applied to a thin disc as well as a fine wire. If a circle of thin sheet copper of thickness x is placed between two optical flats of quartz and the assembly heated under a known weight, the disc would spread or shrink until

$$w = \pi r y (1 - 2r/x) = -2 \pi r^2 y/x \quad \text{very nearly.}$$

This method of measuring y would have a distinct advantage over the one discussed above in that a stable equilibrium is approached. The effect of friction could be determined by approaching the equilibrium from both sides in successive experiments, plotting r as a function of time and extrapolating to $t = \infty$. For a disc one centimeter in radius by 0.01 centimeter thick, w would be about 800 grams, which brings out another advantage of this approach.

The time for appreciable deformation would be difficult to calculate, but one would not expect it to differ by more than one

or two orders of magnitude from the times for extension of thin wires. As the viscosity is an exponential function of temperature, it is reasonable to assume that satisfactory experimental conditions could be set up. It is improbable that the data could be made to yield viscosity coefficients.

A major drawback of this method is that the interface is not copper-copper vapor, but copper-quartz. If copper does not wet quartz, and there is no mutual adsorption, the energy of the interface is equal to the sum of the surface energies of copper and quartz. Let the mechanical equilibrium be upset by the addition of an increment of load dw. If the second order differential change in area of the edge of the disc is neglected, the result will be the appearance of ds centimeters^2 of copper-quartz interface and the disappearance of an equal area of quartz-gas surface. Under the assumption of no adsorption, $dF_{cq} = dF_{cg} + dF_{qg}$, so the qg and cq terms cancel and the experiment gives the true surface tension of copper. There is no way of checking the assumption directly. It is likely that the copper surface at 1000°C will be free of silicon dioxide in an evacuated system, but the non-adsorption of copper vapor on silica is more doubtful.

If the experiment is to be conducted, it should be repeated between flats of other substances, such as fused alumina and graphite. Mutual agreement will indicate that a fairly reliable method is being used.

4. The Bulge Method

A method of measuring the surface tension of copper is suggested by analogy to soap-film experiments. If a circular diaphragm of copper foil is put under a differential pressure, it will, of course, tend to bulge. Gibbs[35] shows that as long as the pressure difference is less than that required to produce a hemisphere, a stable equilibrium is approached. The amount of bulge is readily calculated, as at equilibrium:

$$\gamma ds = pdv$$

If r is the (fixed) radius of the orifice over which the diaphragm is stretched, then

$$s = 2\pi(r^2 + h^2)$$

$$ds = 4\pi hdh$$

$$v = \pi h(h^2 + 3r^2)/6$$

$$dv = 1/2 \, \pi(h^2 + r^2)dh$$

Equating the differentials and simplifying gives:

$$\gamma = \frac{p(h^2 + r^2)}{8h}$$

To produce a bulge of 0.25 centimeter in a diaphragm 2 centimeters in diameter would require a pressure of 2260 dynes per centimeter^2, measurable with considerable accuracy at low absolute pressures. As the edges of the foil are restrained, the thickness does not enter into the calculation, and the foil may be made sufficiently thick to avoid rupture under the stresses of surface tension. The amount of bulge could be measured at room temperature and corrected for thermal contraction.

The above considerations may be summarized as follows:

1. The measurement of surface tension of solid copper is feasible, and sufficient variety of experimental methods exist or can be devised, so that experimental difficulties should not prove insuperable.

2. Attacking the problem as one in mechanics is more promising than the thermodynamic approach.

3. Of the mechanical approaches, one based on balancing with suspended weights the force of surface tension in fine wires is most favorable.

4. A thermodynamic approach based on the vapor pressure of fine copper powder is also feasible.

5. A high vacuum furnace is essential to any of the experiments. It should be capable of holding $1050 \pm 1^{\circ}C$ for long periods of time.

On the basis of these analyses, it was decided to conduct a series of experiments using copper wire.

IV. Experimental Procedure

A. Apparatus

Fine wire specimens could possibly be tested either by
continuous observation at temperature, or by measuring the length
of the wires before and after exposure to the test conditions. The
former method would give a clearer insight into the mode of flow,
but would have no particular advantage in determining the null point
from which surface tension is calculated. On the basis of preliminary
experiments, which will.be discussed in the next section, it soon be-
came evident that the second method was the more feasible one.

A sectional view of the furnace is shown in Figure 5. The
furnace was designed to work at temperatures below the melting point
of copper, and winding calculations were made for $1100^{o}C$. In de-
signing the furnace, cognizance was taken of the fact that it should
be adaptable to the more practical of the other types of experiments
considered, and should also be usable for vacuum and controlled at-
mosphere sintering of fairly massive compacts. The latter con-
sideration led to the use of the long water jacket at the left end,
(for cooling effluent gases) and the installation of a high-speed
vacuum system of considerably higher capacity than would be re-
quired for the wire testing. Otherwise, the design was based on
the testing of fine wires.

A seamless drawnInconel tube, a gift of the International
Nickel Company, was used as the vacuum-tight core of the furnace.
To eliminate any possibility of collapse of this tube under atmos-
pheric pressure, the casing of the furnace was also constructed

Figure 5:   VACUUM FURNACE

     (1) Inconel tube
     (2) Water jackets
     (3) Tapered nichrome resistance heater.
     (4) Alundum cement
     (5) Alundum tube
     (6) Insulating refractory
     (7) Crumpled aluminum foil
     (8) To diffusion pump
     (9) To water aspirator
   (10) Sylphon expansion joint
   (11) Steel outer shell
   (12) Neoprene gaskets
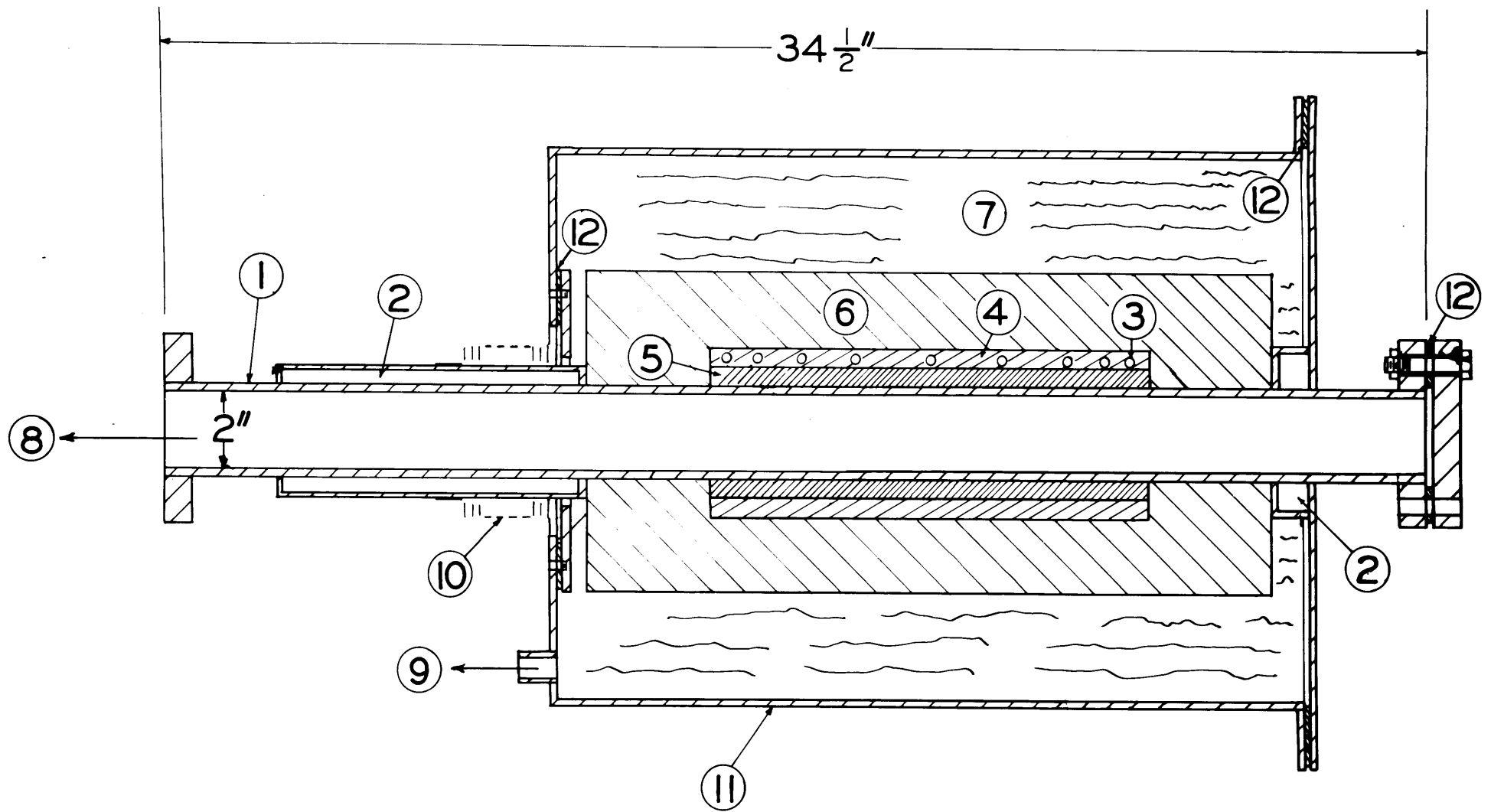
reasonably vacuum tight, and was evacuated with a water aspirator. The chief aim in the design was to obtain a zone about six inches long which could be held uniform to $\pm$ 1°C, so that a group of specimens within this zone would be exposed to not only a constant but an essentially uniform temperature. Thus the windings were distributed over twelve inches, and spaced in accordance with the calculated heat requirements for each inch. Three independently controlled windings were used.

The actual calculations will be found in Appendix F; they are given in outline below.

Consideration was given to the use of concentric radiation shields as thermal insulation. The advantage is that such a system has very low heat capacity and can be heated and cooled rapidly. Calculations showed that such a scheme is ineffective both because emissivity increases with increasing temperature and because of the fourth-power increase of radiant heat transfer with increasing temperature.

Accordingly, a compromise was developed. Two inches of insulating brick were used to drop the temperature to a point where radiation shielding was practical, and the remaining space, 4 1/2 inches, was filled with loosely crumpled aluminum foil. The foil was assumed to be equivalent to three concentric cylindrical shields, which resulted in a radial heat loss at 2500°R of 1150 B.t.u. per hour, as compared to 3900 B.t.u. per hour for radiation shielding only.

There are two components of axial heat loss, conduction along

the tube and radiation to the cold portions of the tube. An exact solution of this situation is possible, but is not necessary. It was merely assumed that the two effects were additive. The hot-zone was approximated by a spherical black body, 2 inches in diameter, radiating to a 4 inch tube which varied from $500^{\circ}R$ at the cold end to $2500^{\circ}R$ where it joined the sphere. The median core of the hemisphere intersects the cylinder on an isothermal circle at $2100^{\circ}R$, and it was merely assumed that the entire sphere radiates to this temperature. On this basis, the axial radiation loss is 2960 B.t.u. per hour.

Calculation of the axial conduction loss is relatively simple, as the cold ends are held at $100^{\circ}F$ by the water jackets. The only value of thermal conductivity of Inconel found in the literature was for $100-212^{\circ}F$, but conductivities of highly alloyed metals decrease only slightly with increasing temperature, and the stated value, 104 B.t.u. per square foot per hour per $^{\circ}F$ per inch thickness was taken to hold over the entire temperature range. This gave a loss of 1200 B.t.u. per hour by conduction. There are no convective losses, as both tube and jacket are evacuated. Thus, the sum of the heat losses at $2500^{\circ}R$ is 5310 B.t.u. per hour, equivalent to 1550 watts.

It was gratifying to find that the actual power required to hold $1050^{\circ}C$ $(2380^{\circ}R)$ was 1400 watts; this despite the extreme approximation made in neglecting the perturbations of the two axial losses on each other.

It was decided to use three 600 watt windings of Tophet A at an element burden of 10 watts per square inch. Paschkis[36]

recommends a maximum burden of 6 watts at a charge temperature of
1850°F, but the author has designed and operated several laboratory
furnaces to operate at this temperature with a burden as high as
12 watts per square inch. Furthermore, the full capacity of the
windings is used only during heating up. At 1550 watts operating
power, the burden would be 8.2 watts per square inch. The commercial
size wire most nearly satisfying these conditions is 18 gauge in
50.5 foot lengths, giving a surface burden at 600 watts of 9.2 watts
per square inch. It was close wound on a 3/16 inch mandrel and
stretched in accordance with the taper calculated in Appendix F.

The tapered coil was wound, three turns per inch, on a 2 1/2
inch by 12 inch alundum tube. The windings were covered with RA98
Alundum cement. Power leads of 11 gauge nickel were welded to the
winding ends and conducted to the casing wall in alundum tubes.
Power was led into the casing through commercial porcelain stand-
off insulators. The temperature control system is discussed in
detail in Appendix F. Once the currents in the three windings are
adjusted, it is possible to hold a five inch zone uniform to $\pm 2^{\circ}$C.
The center of this zone can be controlled to $\pm 1/2^{\circ}$C if the controller
is attended to hourly, but shows a drift of $\pm 3^{\circ}$C over long unattended
periods, due to poor voltage regulation on the power mains. The
vacuum system, also discussed in Appendix F, is capable of maintain-
ing a pressure of about 3×10^{-5} millimeters, as measured by a Cenco
Catalog No. 94180 Thermocouple Vacuum Gauge. This pressure is near
the lower limit for such a gauge, and is uncertain to ± 100 percent.
However, it was always well below the decomposition pressure of

cuprous oxide, as calcualtions (See Appendix C) show that at 827°C, some 100° below the contemplated range for experimentation, the decomposition pressure is already up to 10^{-2} millimeters. Cupric oxide is unstable with respect to cuprous oxide at these temperatures.

B. Materials

Two sizes of wire were used, 36 gauge thermocouple grade copper wire which was on hand in the laboratory, and 40 gauge wire (OFHC) supplied by the General Radio Company. The mean diameter of the former was determined as follows: 25.28 ± 0.04 centimeters of the wire was weighed on a chainomatic balance accurate to ± 0.03 milligram and readable to ± 0.05 milligram. This wire weighed 29.20 ± 0.05 milligram, corresponding to a volume, at density 8.93 grams per cubic centimeter, of 0.00327 cubic centimeter. From the length and volume the diameter was calculated to be 0.0128 ± 0.0001 centimeter. The nominal diameter of B. & S. #36 wire is 0.01270 centimeter. When viewed on the screen of a projection microscope, the diameter of the wire proved to be uniform to ± 0.0003 centimeter, the limit of accuracy of the vernier stage.

The diameter of the 40 gauge wire was determined in a similar manner. 52.9 centimeters ± 0.1 centimeter weighed 22.75 ± 0.05 milligrams. This indicates a diameter of 0.0078 ± .0001 centimeter, as compared to a nominal diameter of 0.007988 centimeter.

It may be well to mention at this point that no such accuracy was possible in the determination of diameter after testing. It can only be said that the specimens were uniform and unchanged to ± 0.0005 centimeter.

Copper weights ranging from 4 to 60 milligrams were used. They are melted in a depression in a charcoal block, using an oxy-acetylene flame as a source of heat. The flame is removed and just before the droplet freezes the end of the specimen wire is thrust into it.

C. Experimental

A series of eight preliminary experiments indicated that:

1. It would be necessary to mount the specimens in a nearly tight copper chamber (Figure 6) to minimize evaporation of the wires.

2. The rate of creep is tremendously less than that indicated from equations (16) - (18), page 30, so accurate length measurements would be required.

3. Chrome plating the ends of the specimens to delineate a gauge length introduces chromium vapor into the system, resulting in surface contamination.

4. The specimens can not be demounted for measuring their length without plastically deforming them.

These eight tests are discussed in greater detail in Appendix G. From them the following experimental technique was developed.

The wires are cut about five centimeters long and a knot is tied about two centimeters from one end. The weights are welded to this end, and the free ends passed upward through the holes in the lid. The ends are bent over and taped down with scotch tape and the specimens are carefully straightened.

Figure 6:   COPPER CELL WITH THERMOCOUPLE WELL

$1\frac{9}{16}$

$1\frac{7}{8}$

$1\frac{3}{8}$
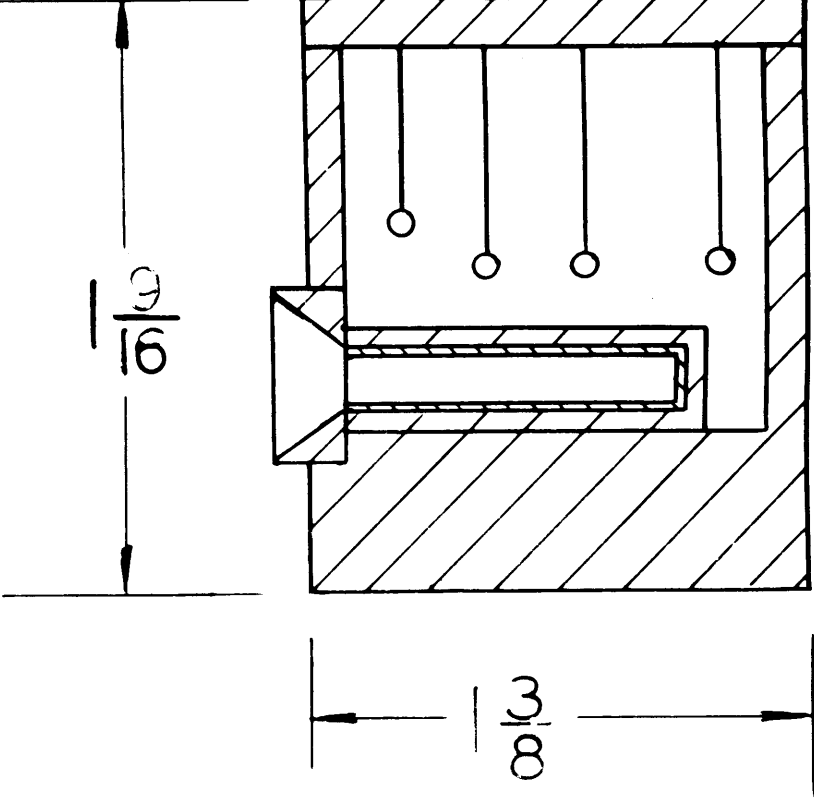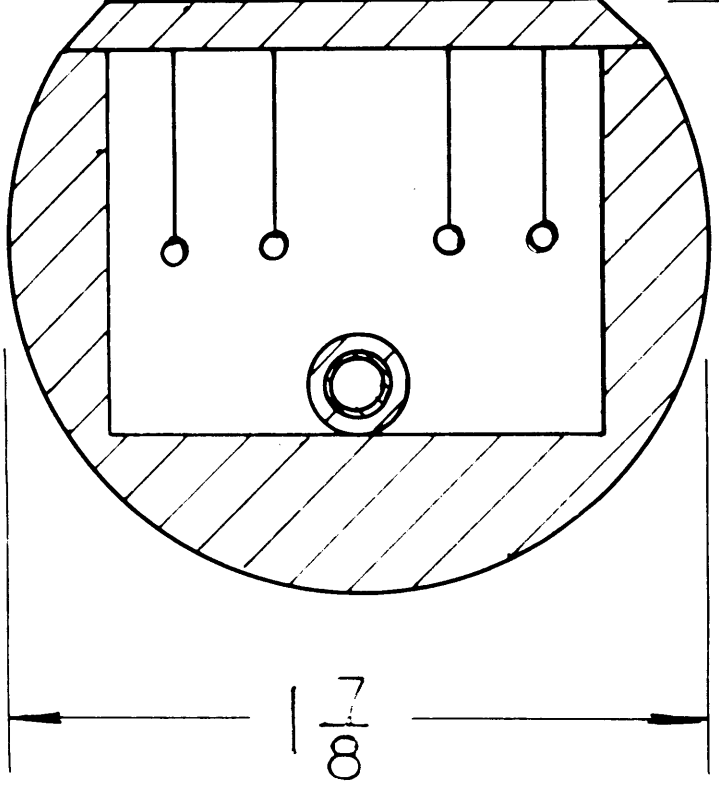
The lid, with eight specimens so mounted, is placed on the cell and taped down, and the assembly is inserted into the cold furnace. The furnace is sealed and evacuated, and the power turned on. The tape carbonizes, of course, but by the time it has lost its holding power, the wires will have softened sufficiently so that they stay in position. The annealing period is one to two hours at 1025°, and the assembly is furnace cooled in vacuo.

The primary purpose of the anneal is to allow any dimensional changes due to recyrstallization and grain growth to take place before the specimens are measured. Also, during the anneal the free ends of the specimens sinter to the lid, and the knot becomes self-welded at its cross-over points.

The lid is removed from the cell and set on a rigid support, with the specimens hanging free. A Cenco Measuring Microscope, Catalog No. 72935, is used for length measurements. This microscope is similar to a cathetometer, except that the optical system consists of a 40 power microscope instead of a telescope, and the vernier scale is only 16 centimeters long. The measurement is made between the bottom intersection of the knot with the specimen wire, and the intersection of the wire with the weight, as viewed from a fixed direction. The length measurements made this way are reproducible to ± 0.001 centimeter. As a precaution against rotation of the specimen during test, each knot is sketched as it appears in the microscope field, and if any assymmetries exist in the weight, these are also sketched. However, no change in shape or appearance of either was ever noticed.

The lid is next very carefully put back on the cell, and the assembly is returned to the furnace. An experimental run may last from 24 to 150 hours, depending on the temperature. Heating-up time is 1 1/2 hours, and at the end of the run, the furnace is allowed to cool overnight. It takes some 15 minutes to heat from 25° below test temperature to the operating temperature, and after shut-down the furnace cools 25° in 7 minutes. Since the strain rate nearly doubles for a 25° increase, the heating and cooling times can be neglected.

The cold assembly is removed from the furnace and the wires again measured. The weights are detached and weighed to $\pm$ 0.05 milli-gram. The length change is converted to ordinary strain and the weight to ordinary stress in dynes per centimeter^2.

Consideration was given to the possibility of anamalous end effects occuring at the junction between the wire and the weight. To test for this, a second knot was tied just above the weight. (Figure 7) Lengths were measured both between the knots and from the upper knot to the weight. Strains determined from the two sets of measurements checked to within the instrumental accuracy. How-ever, this practice was continued, as it gave a double measurement of the least certain parameter in the experiments. In the last ex-periment, test No. 16, a Gaertner measuring microscope was used. This instrument is also built on the cathetometer principle, but has a micrometer screw drive accurate to 0.0001 inch (or 0.0003 centimeter instead of 0.001 centimeter.)

The experimental results are summarized in Table I.

Figure 7: TYPICAL SPECIMEN

Arrows show gauge points.
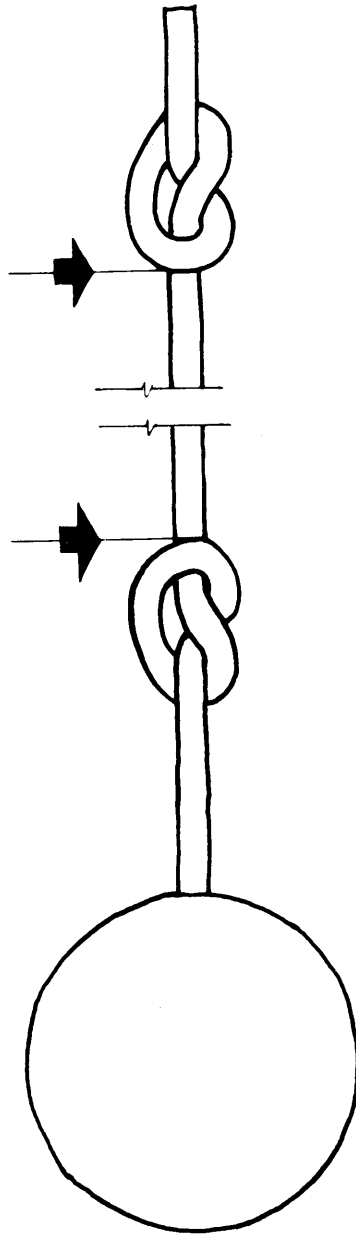
TABLE I

Test No.	9		10		11		13		14		15		16	
Temperature °C	1024		999		950		1049		1050		1000		950	
Time, sec. x 10⁻⁵	1.08		1.80		5.15		.874		1.69		2.80		5.35	
Wire radius cm.	.0064		.0064		.0064		.0036		.0036		.0036		.0036	
Spec. No.	σ	ε	σ	ε	σ	ε	σ	ε	σ	ε	σ	ε	σ	ε
1	.091	-6.1	.069	-4.4	.076	-3.9	.091	-4.5	.096	-8.9	.072	-10.7	*	**
2	.738	-4.5	.076	-4.2	.777	-2.1	.861	-3.5	*		1.179	-5.7	1.706	-3.10
3	1.461	-3.1	1.742	-1.8	1.774	-1.3	1.319	-2.5	2.428	-5.0	2.455	-2.1	3.508	-0.67
4	2.368	-0.6	2.350	-0.5	2.755	+1.3	2.315	-0.5	3.655	-0.8	3.393	-0.9	4.107	-0.32
5	2.535	-0.0	2.807	+0.6	2.313	-0.6	2.865	+1.3	4.545	+3.1	3.635	-0.6	5.459	+2.00
6	3.145	+3.7	3.180	+3.0	3.140	+1.9	2.842	2.4	5.047	4.1	4.235	+0.2	5.724	3.22
7	3.472	4.2	3.810	2.3	3.465	2.1	3.520	3.8	*		5.540	4.6	6.682	4.89
8	4.644	3.8	4.603	5.9	4.547	4.1	4.545	5.4	7.530	9.3	8.135	9.1	8.345	6.30

Stress dynes/cm² x 10⁻⁵, Strain x 10³

* Specimen damaged during measurement

** Measuring microscope accurate to ± 0.0003 cm. used in Test number 16

Test number 12 was an unsuccessful attempt at making a run at 1060°C. The weights are not oxygen-free, and they melted and dropped off.

Equations (15) and (16), page 29, can be simplified by expressing them in terms of stress and strain. They then become:

$$\frac{d\varepsilon}{dt} = \frac{1}{6\eta} (\sigma - \gamma/r), \text{ and}$$

$$t = {}^{r_0}/\!\gamma \left[6\eta\varepsilon + r_0 \ln \frac{(\sigma r_0 - \gamma r t)^2}{(\sigma r_0^2 - \gamma r_0)} \right]$$

where $r_t = {}^{r_0}/\!\sqrt{\varepsilon + 1}$

For the small strains shown in Table I, it is not necessary to use the integrated form. The differential form becomes:

$$\varepsilon = \frac{t}{6\eta} (\sigma - \gamma/r)$$

To **recapitulate:**

ε = ordinary strain

η = viscosity

σ = ordinary stress due to the appended weight only

r = the radius of the specimen

For a uniform set of wires this yields a linear relationship between stress and strain of slope $t/6\eta$, with an $\varepsilon = 0$ intercept at $\sigma = \gamma/r$. (It is interesting to note that this intercept represents a singularity in the integrated equation. See Figure 4.) The data in Table I is plotted in Figures 8 - 14, and it can be seen that a straight line represents this data as well as any other simple

Figures 8 - 14:   STRESS VERSUS STRAIN IN WIRE SPECIMENS

Circles represent Least Square intercepts

STRAIN

STRESS DYNES PER CM^2

5×10^5

TEST NO.9

STRAIN

.006

.004

.002

0

-.002

-.004

-.006

1   2   3   4   5X10^5

STRESS DYNES PER CM^2

TEST NO. 10

STRAIN

.006

.004

.002

0

-.002

-.004

-.006

1

2

3

4

5×10^5

STRESS DYNES PER CM^2

TEST NO.11
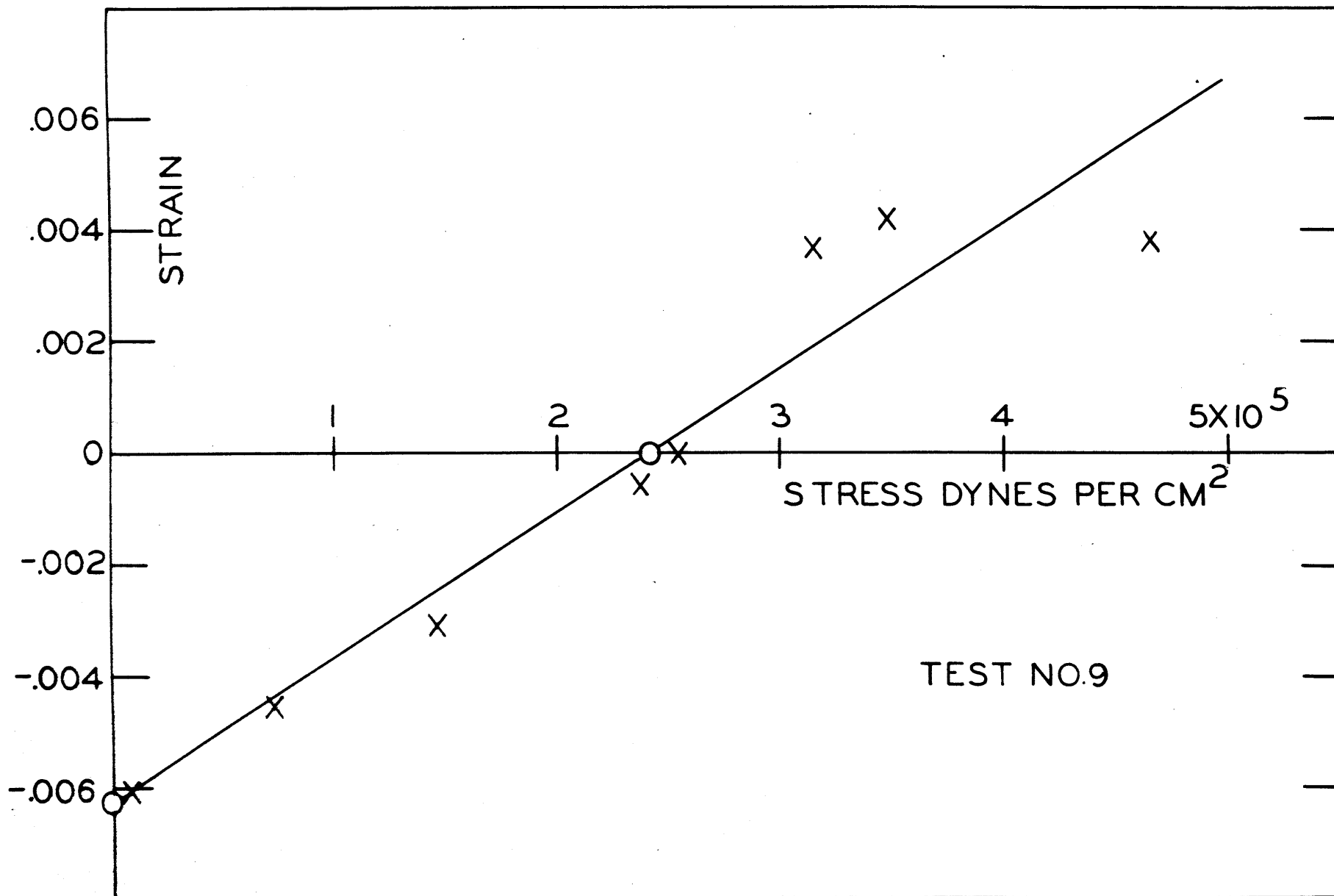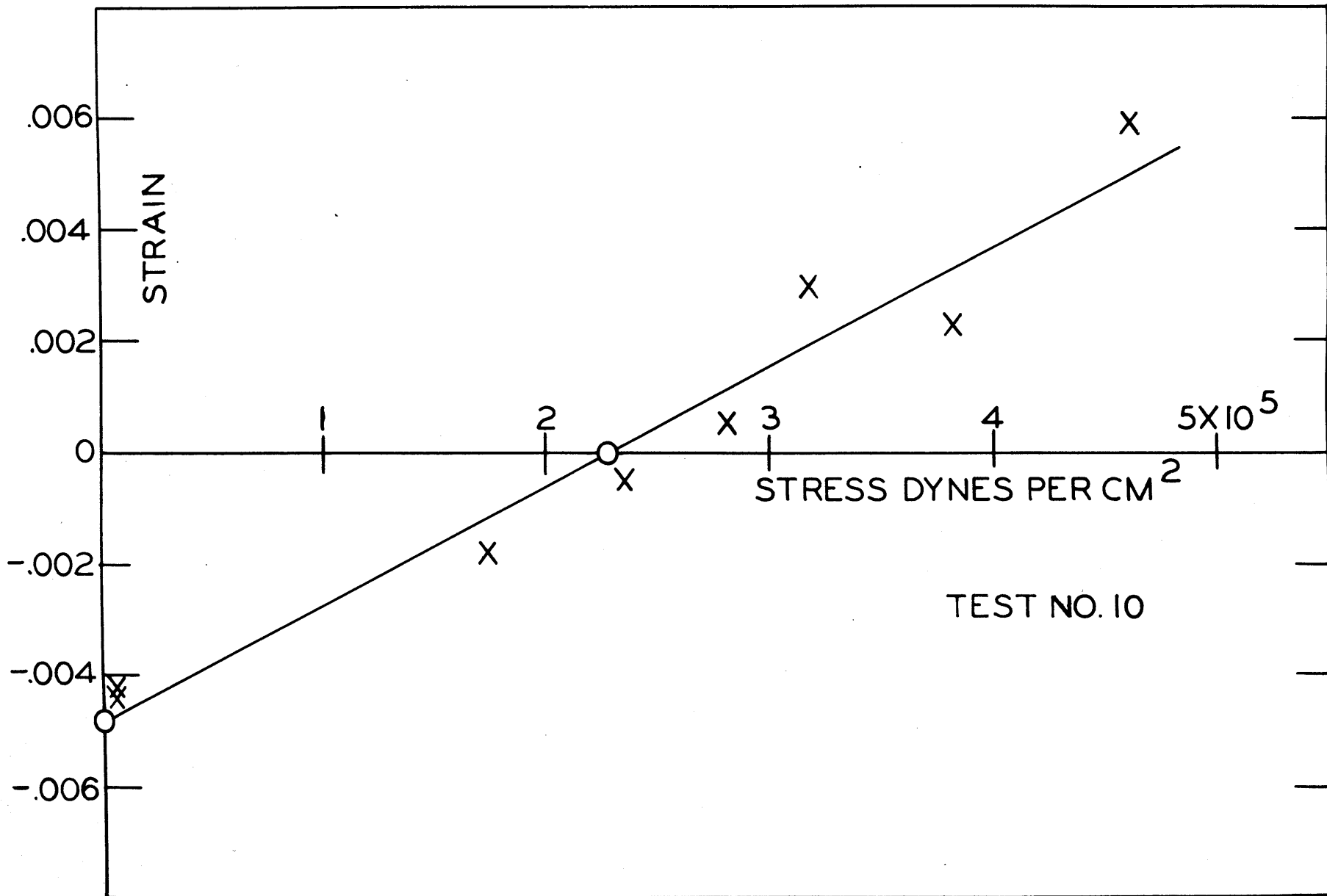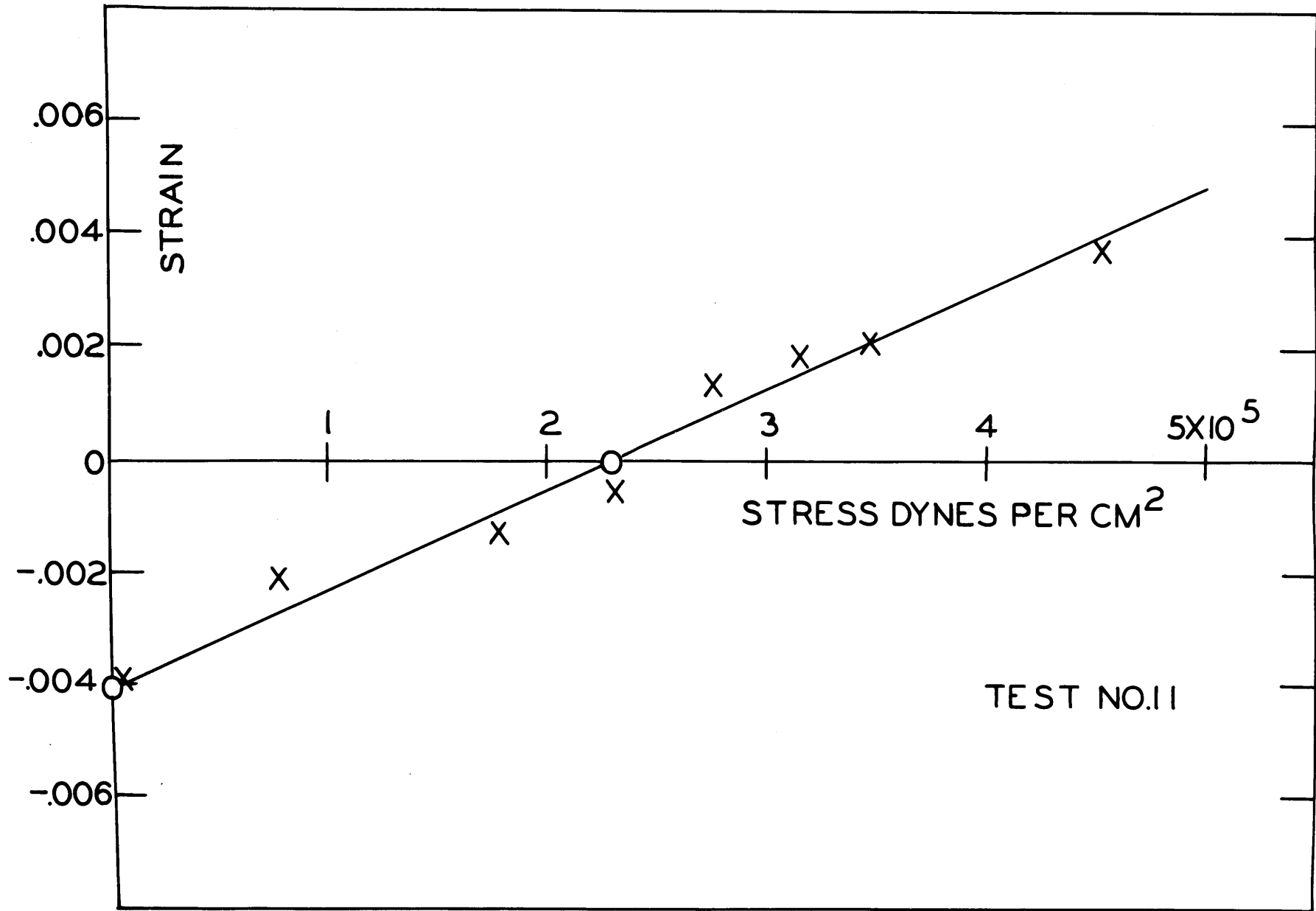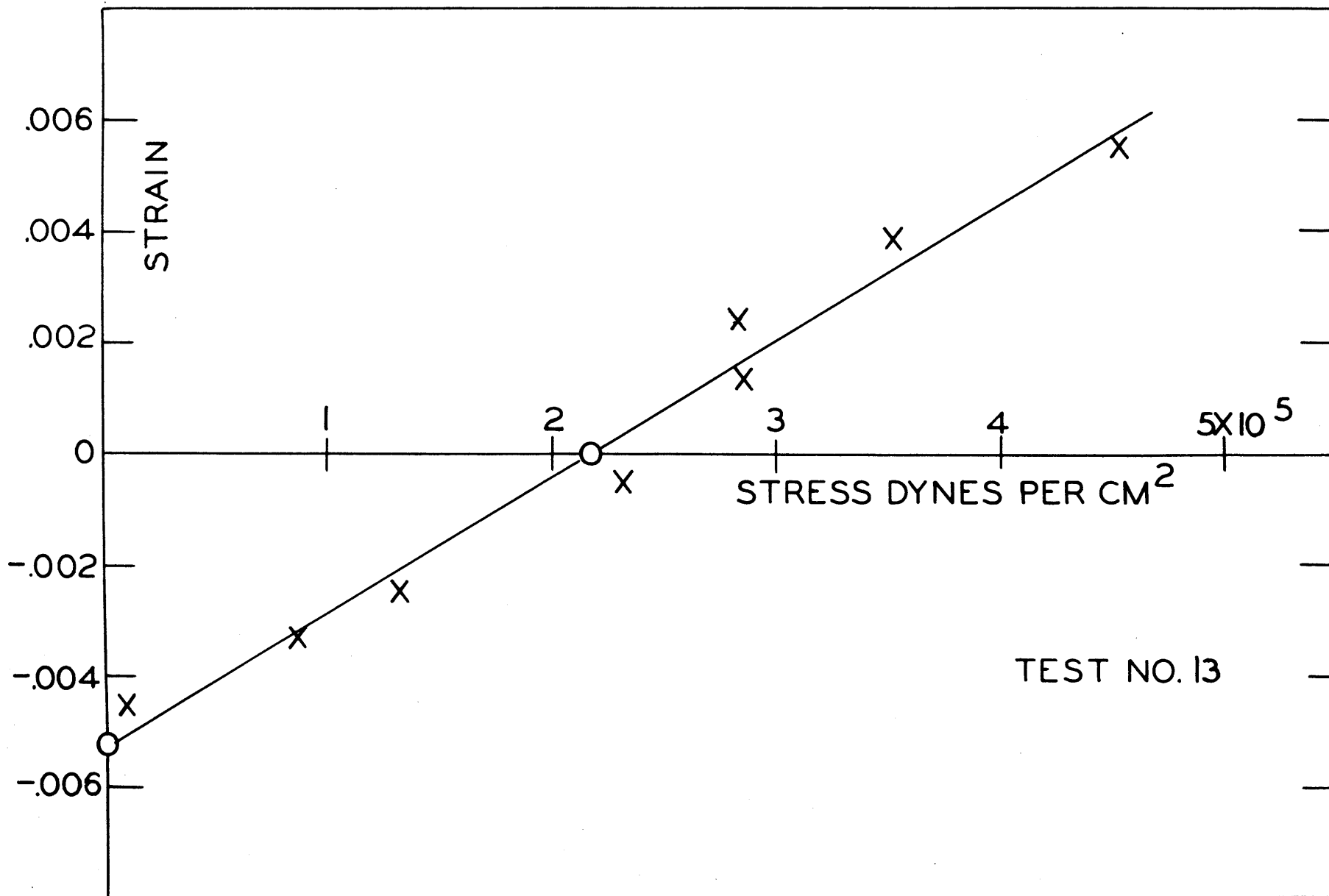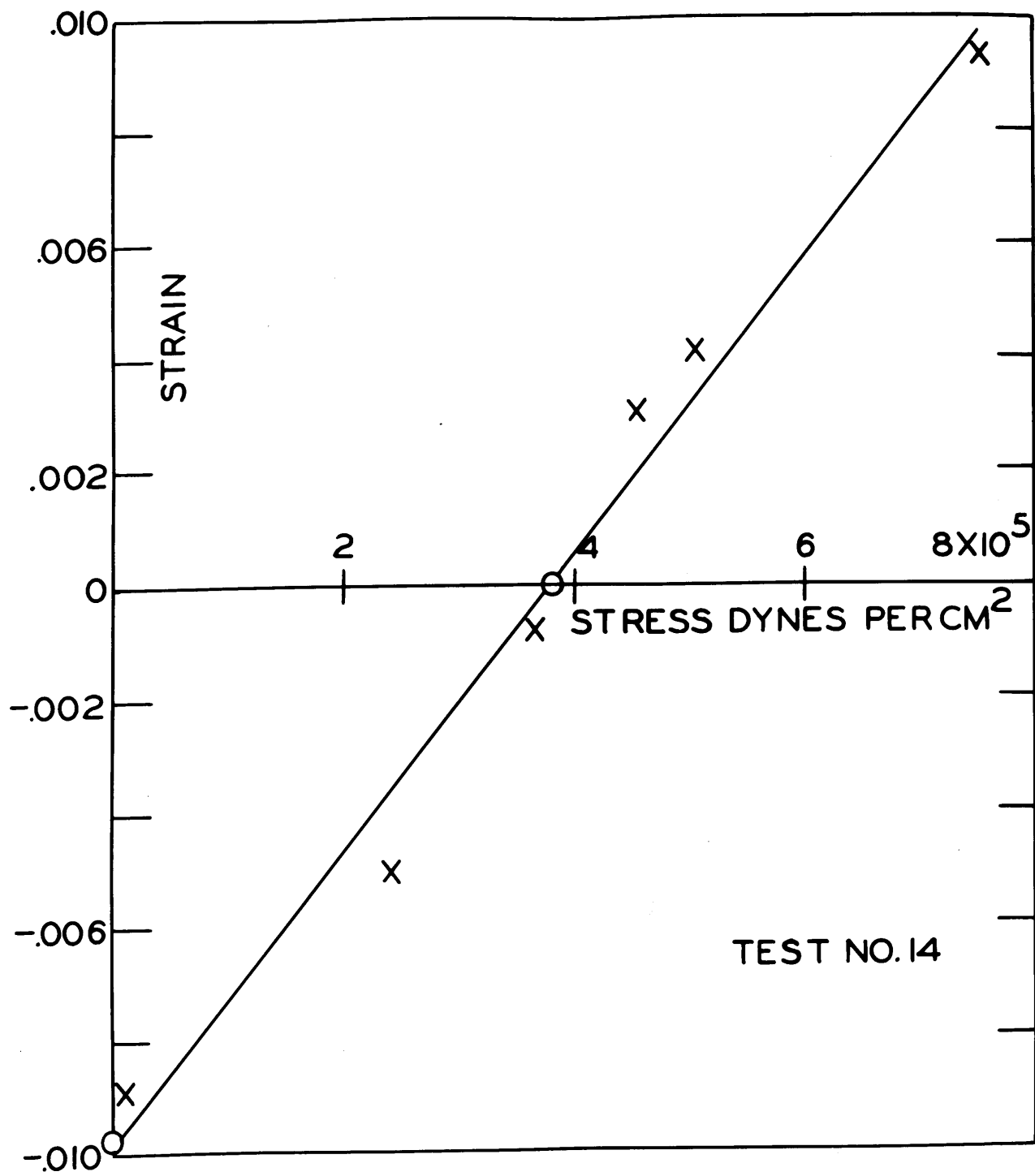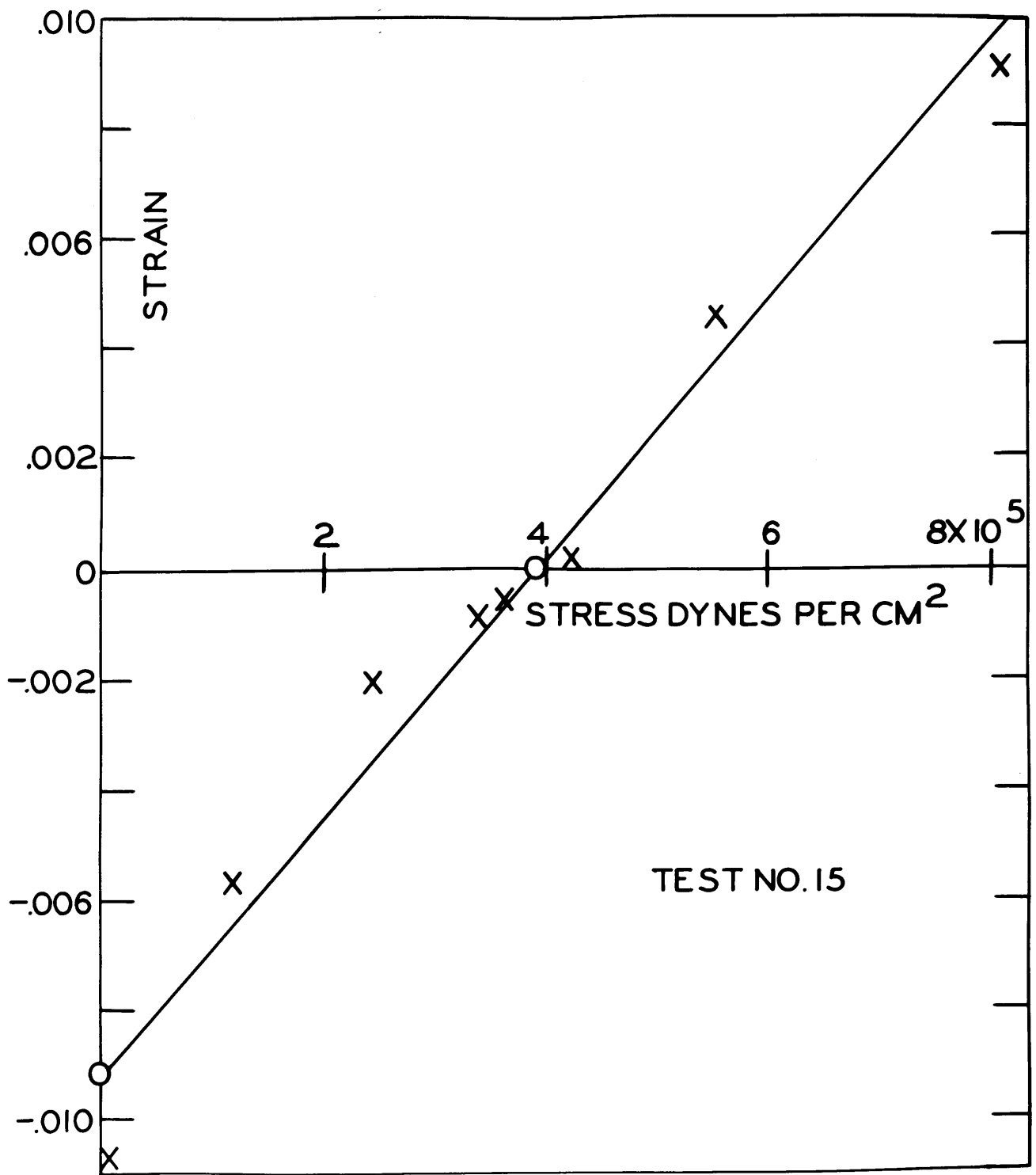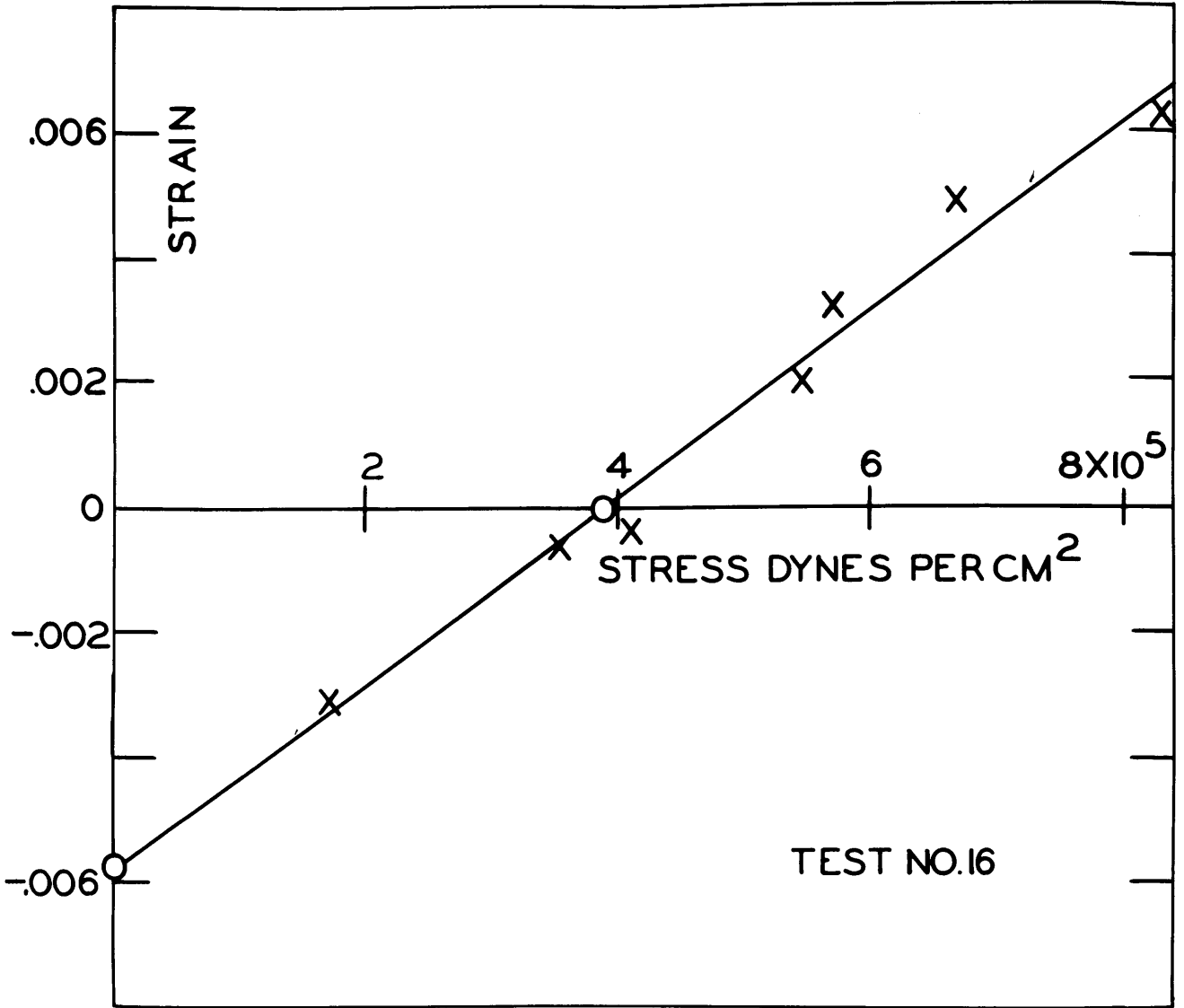
curve. The intercept and slope of this straight line are calculated by application of the method of least squares.[43] Surface tension is calculated from $\gamma = \sigma_\gamma r$, where σ_γ is the value of applied stress at the $\mathcal{E} = 0$ intercept.

In Figure 15, the surface tensions determined from this relationship are plotted against temperature. If the anomalous point at $1025^\circ C$ is ignored, a value of 1370 dynes per centimeter at the melting point is obtained. The temperature coefficient is -0.46 dynes per centimeter $- {}^\circ K$, which is consistent, as is to be expected on theoretical grounds[16][41], with an extrapolation to zero in the neighborhood of the critical temperature.

D. Precision of the Results

The precision of a physical constant can be determined in several equally valid ways. For this research, the author prefers to proceed as follows:

(1) Take the sum, without regard to sign, of the stress deviations in each of the graphs, Figures 8 - 14.

(2) Determine the probable error (P.E.) in each of these curves by dividing this sum by $n^{3/2}$, where n is the number of specimens.

(3) Express this as a percentage error in terms of σ_γ, the stress-axis intercepts in Figures 8 - 14.

(4) Recalling that $\gamma = \sigma_\gamma r$, and that the error of a product is the sum of the errors of the individual factors, determine the probable error in γ, the surface tension.

Figure 15: THE TEMPERATURE DEPENDENCE OF SURFACE TENSION

OF SOLID COPPER
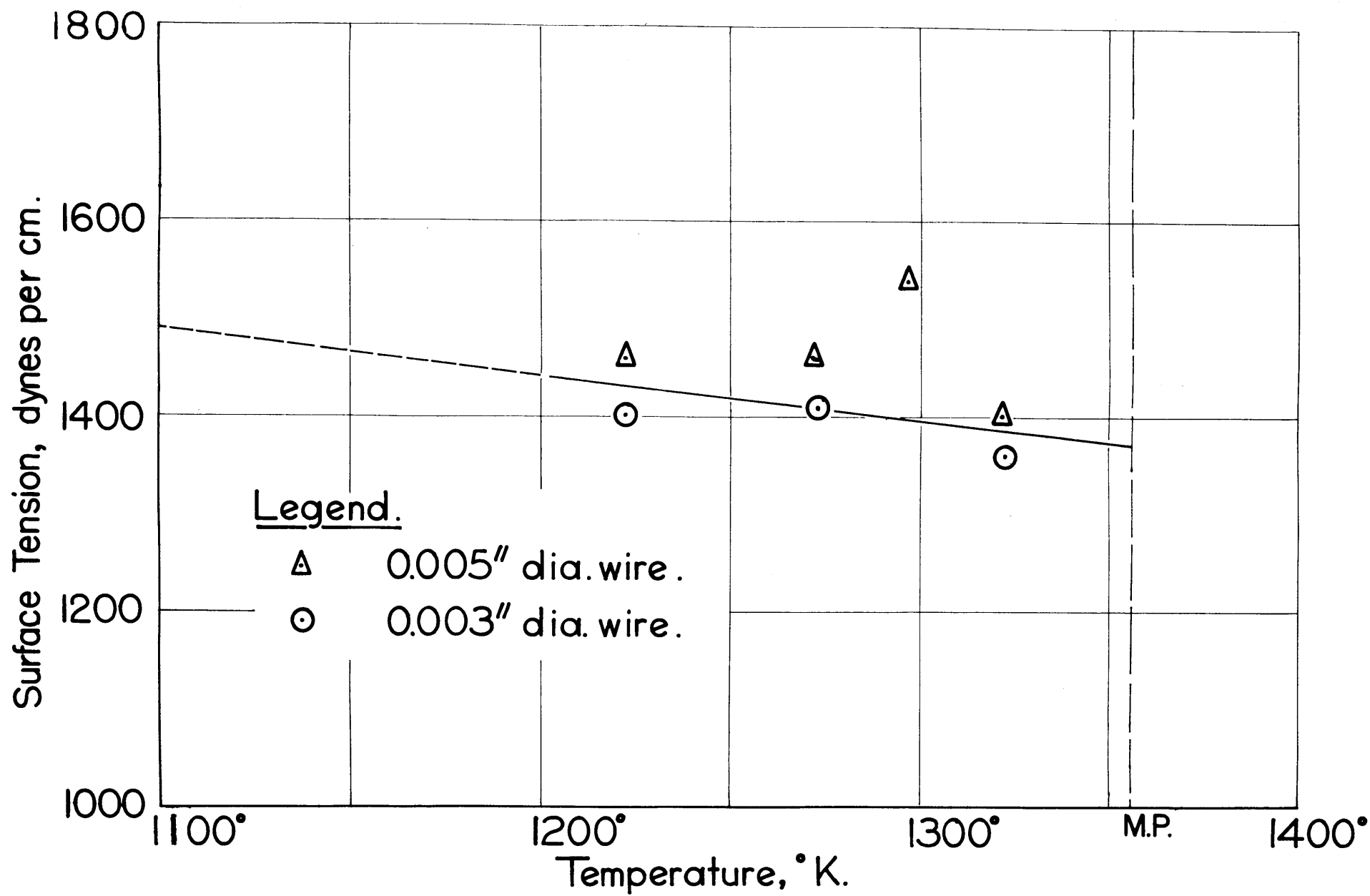
The author prefers this graphical method because it implicitly includes all the random errors, not just the ones that can be numerically evaluated. It includes as well the relatively large systematic (that is, non-random) error in the measurement of the diameter. (This is a systematic error because if an individual wire is somewhat smaller than the measured value, it is probable that all wires from the same source will be smaller to much the same degree).

The results are as follows:

TABLE II

Test No.	Fractional P.E. of σ_y	Fractional P.E. of r*	Fractional P.E. of γ	γ (dynes/cm.)	P.E. (dynes/cm.)
9	.051	.039	.090	1560	± 140
10	.053	.039	.092	1460	± 130
11	.033	.039	.072	1460	± 100
13	.033	.039	.072	1400	± 100
14	.039	.064	.103	1360	± 140
15	.032	.064	.096	1410	± 130
16	.026	.064	.090	1400	± 130

* See page 39

Thus, for example, in Test number 13, the surface tension of the 36 gauge copper wire at 1049°C is found to be 1400 ± 100 dynes per centimeter, and in Test number 14, 40 gauge wire at 1050°C has a surface tension of 1360 ± 140 dynes per centimeter.

It is no coincidence that the fractional probable error in the intercept is of the same order of magnitude as the uncertainty

in the diameter. The average change in length of a specimen is about equivalent to one diameter. Thus, both uncertainties can be traced in large part to the uncertainties in the optical measurements.

The final expression for surface tension:

$$\gamma = 2000 - 0.46 \, T$$

valid between 1200 and 1350°K, is better than any of the individual determinations of γ; theoretically it is $\sqrt{7}$ times better. However, it is safer to assign an uncertainty of ± 100 dynes per centimeter to the surface tension for copper derived from this expression.

The average deviation, or "scatter", in Figure 15 is considerably less than the Probable Error, since systematic errors will not appear in this scatter. It will be seen that the average deviation in Tests number 10 - 16 is only 26 dynes per centimeter while Test number 9 deviates 125 units from the straight line. Such an observation may be legitimately rejected.[42]

E. The Viscosity of Copper

As indicated in the introduction, the purpose of this work was to develop an experimental method for the measurement of the surface tension of solid metals. The results on viscosity are a by-product and, though interesting, should be considered incomplete.

Viscous flow is defined phenomenologically as a process in which strain rate is proportional to applied shear stress. Recent theory of condensed systems includes the further criterion that the

flow must be atomic as well. Steady-state creep is often termed
"quasi-viscous" in that the true strain rate, while not proportional
to the applied stress, is constant for a constant true stress.
Kauzmann[37] points out that another mode of flow may exist in
metals, which involves the motion of blocks rather than single
atoms, but which is otherwise proportional to the applied shear
stress at least at low stresses.

Kauzmann's analysis of viscous flow leads to the expression

$$\eta = \frac{\lambda L \, k \, T}{2qA \ell D} \tag{1}$$

where L = spacing between flow lamellae, normal to flow direction

    λ = relative motion of adjacent lamellae, per unit process

        of flow

    q = stress concentration factor, = 1 if no part of the fluid

        can support shear

    A = area of a unit lamella of flow

    ℓ = distance between normal and activated state of the flow

        unit

"D" is the coefficient of self-diffusion of the material, if the
mechanisms of self-diffusion and of viscous flow are identical.
It is only required that the mechanisms correlate. It is not nec-
essary that every unit involved in diffusion be also involved in
viscous flow.

For an atom-wise process of self-diffusion, $\lambda = L = (A)^{1/2} = 2\ell$.
For an atom-wise process of viscous flow under very slight shear,

where the probability of a forward jump of an atom exceeds only slightly that of a reverse jump, the relationship $\lambda = 2\ell$ remains valid. Thus equation (1) reduces to:

$$\eta = \frac{kT}{\lambda D} = \frac{kT}{\lambda D_0} e^{\frac{Q_0}{RT}} \tag{1a}$$

where λ is now the interatomic spacing. If the Dushman-Langmuir value for D_0 is inserted, the expression becomes:

$$\eta = \frac{h}{\lambda^3} \times \frac{RT}{Q} e^{\frac{Q}{RT}} \tag{2}$$

In our experiments the flow is viscous, at least to the extent that the data in Table I can be approximated by straight lines; as shown on page 44, the viscosity can be obtained from the slope of such a straight line, according to the equation:

$$\varepsilon = \frac{t}{6\eta} (\sigma - \gamma/r) \tag{3}$$

In Figure 16, the logarithm of the viscosities derived from Equation (3) are plotted against the reciprocal of absolute temperature. The equation of the straight line as drawn is

$$\eta = 130 \, e^{59,000/RT}$$

The activation energy of 59,000 calories per mol is within the range of values reported for self-diffusion of copper[38]. The action constant, however, is 10^7 times larger than that predicted from equation (2). The coincidence of activation energies suggests that the atom or atomic vacancy is the unit of flow, but evidently only a very small fraction of vacancies can participate in the flow.

The divergence in viscosity between the two wire sizes, (see

Figure 16: THE TEMPERATURE DEPENDENCE OF VISCOSITY OF

SOLID COPPER
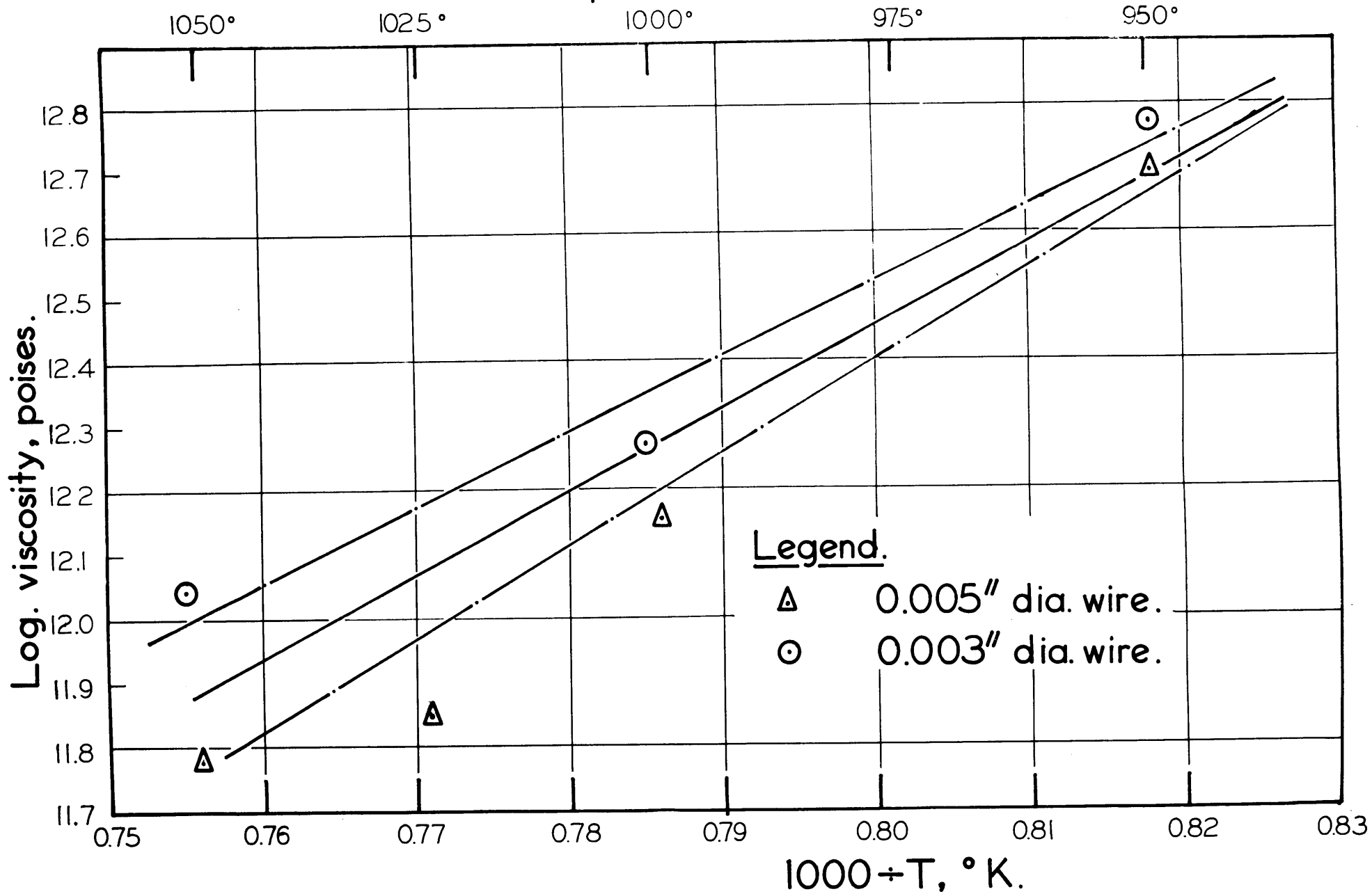
dotted lines, Figure 16), indicates that the surface-to-volume ratio of the specimens may be a factor in determining the flow rate. Apparently, the viscosity of the surface phase greatly exceeds that of the interior of the copper.

The mathematics of this condition has not yet been formulated, nor is the data as yet extensive enough to warrant such formation. Nevertheless, some speculation may be justified.

Surface energy owes its existence to the presence of unsatisfied atomic bonds at the surface. However, if surface tension is calculated by merely summing the energy of these broken bonds, (see page 11), the result is too high by roughly 10 percent[16], because the unsevered bonds in the surface layers of atoms distort in such a way as to take up some of the excess energy. These high-energy bonds might account for a strengthening of the surface layer, according to Benedicks.[39]

In fatigue testing, and tension testing of brittle materials, failure is generally initiated at the surface, and the strength of the surface skin plays an important role, even in large section sizes. Benedicks and Ruben[40] investigated a quenched (untempered) carbon steel immersed in various liquid media, and found the strength to be dependent on the surface tension of the medium.

F. Metallographic Studies

Sectional views of the specimens are shown in Figures 17 - 20.
Mounting and polishing these dead-soft fine wire specimens is a very
difficult job, so much so that it was possible to prepare only one
representative photomicrograph of the 40 gauge wire.

The outstanding feature of these specimens is the long
columnar twinned crystals and the relative scarcity of longitudinal
grain boundaries. The one shown in Figure 17 was the only well-
defined longitudinal bi-crystal noted in the several specimens
examined. The extremely coarse intro-crystalline mosaic pattern,
characteristic of copper heated for long periods at just below the
melting point, is best seen in Figure 20.

Some porosity will be noted on the photomicrographs, the
36 gauge wire showing this possibly to a greater degree than the
40 gauge. How much of this is true porosity and how much a conse-
quence of the great difficulty of specimen preparation, is hard to
say. If it is not due to preparation, the porosity may be a factor
in the scatter of the experimental results. It is probably a con-
sequence of the fact that oxygen-free copper, although it is pore-
free in the as-cast state, does have in solution a small amount of
nitrogen, possibly also of carbon monoxide. From Sievert's Law, one
sees that, in vacuo, the copper will be supersaturated with respect
to these gases, and there might be a tendency for them to come out
of solution within the specimens.

In the photomicrographs presented, and more so in others not
included in the thesis, it was noticed that many of the individual

Figures 17 - 19:   LONGITUDINAL SECTIONS OF 36 GAUGE WIRE

AFTER TEST.

200 X   dichromate etch.

Figure 20:   LONGITUDINAL SECTION OF 40 GAUGE WIRE

AFTER TEST.

200X   dichromate etch.
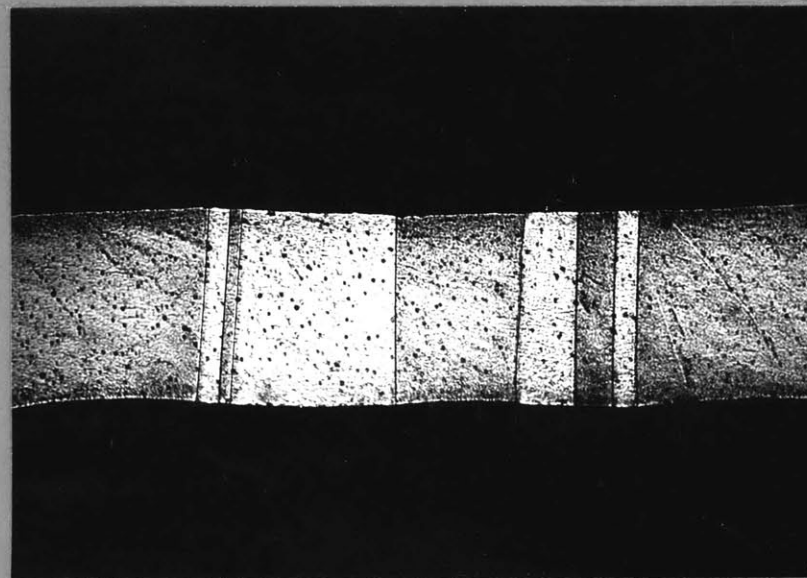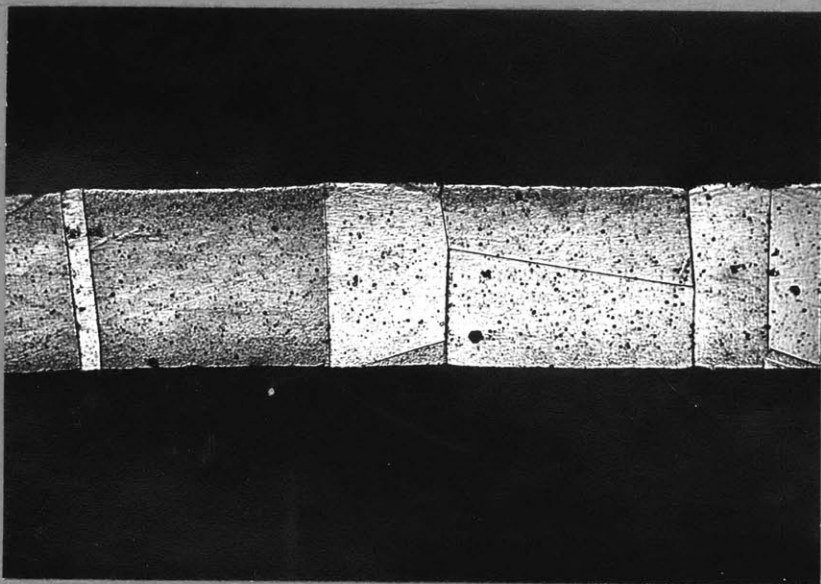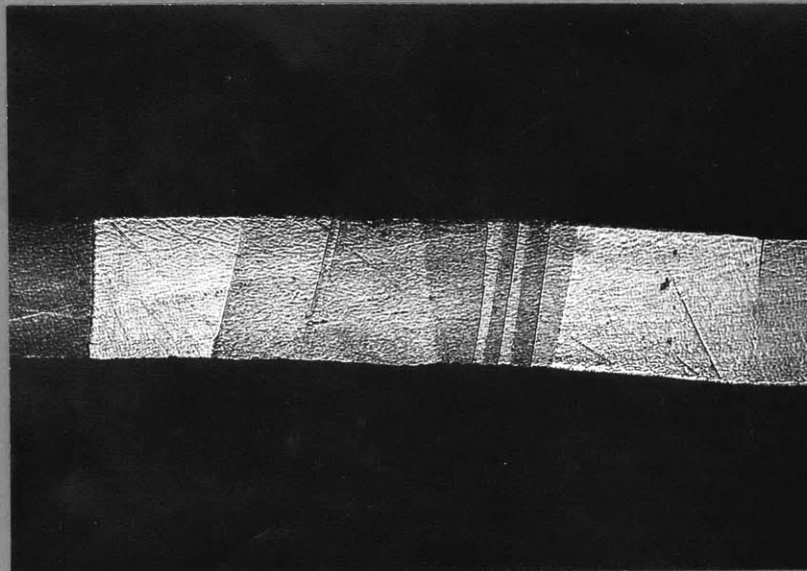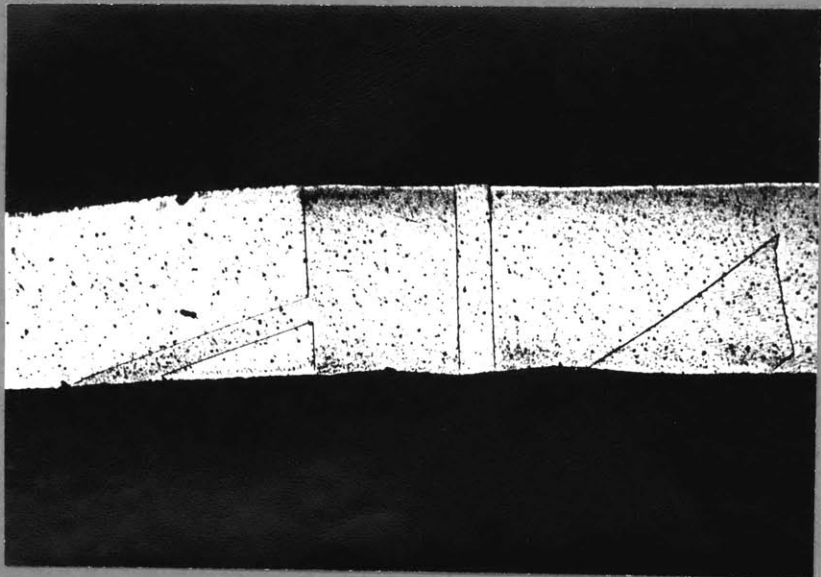
grains are longer than the diameter of the wire. In sheet specimens Beck[55] has stated that the maximum grain size achieved on annealing is seldom greater than the thickness of the sheet.

V. Discussion of Results

A comparison of the experimental value for the surface tension of copper with the value calculated by the Harkins method is of considerable interest. On page 12 the calculated value was given as

$$\gamma = 2170 - 0.53 \, T$$

Extrapolating our experimental value to $0^\circ K$ yields

$$\gamma = 2000 - 0.46 \, T$$

The corresponding values at the melting point are 1450 dynes and 1370 dynes respectively.

This correspondence is of fundamental significance. It shows that a good working value for the surface tension of a solid metal can be obtained by a simple calculation. It also shows that the free-bond concept of surface energy, crude though it may be in comparison to the quantum-mechanical concepts, provides a good empirical jumping-off point for the study of surface tension.

As pointed out on page 12, there is good reason to believe that there is no large discontinuity in the surface tension when the melting point is crossed. There have been a few determinations of the surface tension of liquid copper. Quincke[44], using the drop-weight method, obtained a value of 1163 dynes/cm at 1083°. From capillary rise, Libman[45] obtained

$$\gamma = 1268 - 0.16(T - 1083)$$

where T is in $^\circ C$, and the experiments were conducted between 1100° and 1318°. From maximum bubble pressure, Sauerwald[46] obtained

$$\gamma = 1060 + 0.78(T - 1083)$$

(The writer has taken the liberty of deducing these formulas from the experimental results of the authors).

Sauerwald's positive temperature coefficient makes his results of doubtful value. Such a coefficient could very easily be indicative of desorption of a surface contaminant with increasing temperature. Libman's data indicates a negative coefficient, but a much smaller one than the calculated and experimental values for solid copper, so here again surface contamination is a possibility. It may be well to interpolate here that, since copper is close-packed in both the liquid and the solid state, there should not only be little change in the surface tension during fusion, but also little change in slope in the temperature dependence of surface tension.

Thus the results on liquid and on solid copper are uncertain to the extent that either Turnbull's conclusion that Δf on fusion is of the order of -100 dynes/cm or Frenkel's conclusion that 1 dyne/cm is the approximate value, may be the true one.

VI. Recommendations for Future Work

Four lines of work are suggested. First, the experimental techniques should be refined to the point where the scatter in the stress-strain plots is, if not eliminated, at least traced to something more fundamental than uncertainties in the measurements. Optical equipment is manufactured for measuring a horizontal specimen to $\pm.00001$ cm., and work should be done in adapting such an instrument to vertical specimens. Some preliminary experiments were performed which indicate that a gauge mark can be circumscribed on the wires with a razor blade, without unduly damaging the specimen. Such gauge marks could be sighted to an accuracy of $\pm.0001$ cm., and possibly even more accurately.

Second, the effect of various atmospheres on surface tension should be investigated. A particularly attractive series of experiments would consist in measuring surface tension of copper in various $CO-CO_2$ mixtures at atmospheric pressure. It is unlikely that either of the bulky molecules would adsorb to any great extent at these temperatures. However, one might expect a transition, with increasing CO_2 pressure, from an adsorbed oxygen layer through a chemisorbed layer to, finally, a true Cu_2O phase. The chemisorbed layer may be thought of thermodynamically as a surface-stable but volume-unstable Cu_2O phase. The changes in surface tension with CO_2 pressure, and any discontinuities in this function, would yield valuable data on the thermodynamics of the surface layer.

Third, the surface tension of other pure metals should be determined by the wire technique.

Fourth, the surface tension of some single phase alloy systems should be investigated. The effect of composition on surface tension is a direct measure of the degree of inhomogeneity at the surface of a two-component phase.[48]

Each of the above experiments will also yield additional information on the viscosity of metals. The size effect in flow resistance should certainly be thoroughly investigated, and a correlation sought with Kuczynski's researches on particle size effect in sintering[49]. The latter also found, in fine wires, a variation in elastic properties with wire diameter.[50] This he attributes to different textures in the interior and at the surface. His conclusions should be reviewed if a real and regular variation of flow resistance with diameter is found.

Interfacial tension, a parameter of much more interest to the metallurgist than surface tension, should be investigated. Following is a suggested method for measurement of interfacial tension in the copper-silver system:

The copper-silver system is a eutectic with mutual solid solubility of 8% at each end at the eutectic temperature of $779°$. At $750°$, 7% of Cu is soluble in silver, and 6.5% Ag is soluble in copper.

(1) Electroplate a length of 40 gauge silver wire with copper and heat at $750°$ until the two phases are mutually saturated. This will result in an α solid solution of copper in silver on the inside and an α' solid solution of silver in copper on the outside, separated by a boundary A. The weight of copper to be plated on, such that the core diameter does not change appreciably during diffusion, can be readily calculated from the lever law and the densities of the two phases.

(2) Quench from 750° to make supersaturated α and α'.

(3) In a cyanide bath of proper composition, plate an alloy layer corresponding to α in composition, to a fairly substantial thickness, say 0.005". This will give a second boundary B, and an outer layer of α .

(4) Reheat to 750°.

(5) At predetermined intervals, quench, and cut off a small portion of the composite wire. Measure the areas enclosed by A and by B at several points in the specimen.

Solubility, like any other thermodynamic function, depends on the radius of the dissolving particle. The dependence is readily expressed as a function of the interfacial tension and the radius. Thus the solubility of silver in α' at A is slightly greater than at B. Diffusion will occur under this solubility gradient until the α core disappears. Meanwhile, the area enclosed by B, less the area enclosed by A, remains substantially constant.

This is almost, but not quite, a problem of steady-state diffusion, since the concentration gradient increases as the core becomes smaller. The writer has not yet attempted to set up the equations for dA/dt as a function of γ and the mutual diffusion coefficient of silver and copper, but such a problem should not prove too difficult.

Finally, it might be advisable to state that all future work of this kind should be carried out with wire made from vacuum melted metals.

APPENDIX A   Surface Tension Effects as a Function of Shape

(1)   Vapor Pressure of a Thin Cylinder

It was shown in the body of this thesis that the ratio
of vapor pressure of a sphere to that of an infinite plane surface
is expressed by:

$$RT \ln p_r/p_0 = 2\gamma V/r$$

where V is the atomic volume of the material, and r is the radius
of the sphere. A similar expression for a cylinder is derived as
follows:

Let p_0 be the vapor pressure above an infinite plane
surface, and p_ϕ be that over a cylindrical surface of diameter ϕ.
If dn mol is transferred from the plane to the cylinder, the change
of free energy is

$$dF = dnRT \ln p_\phi/p_0$$

$$\text{but} \quad dF = \gamma ds$$
$$s = \pi \phi l$$

$$ds = \pi \phi dl$$

If V is the molar volume, then

$$nV = \pi \phi^2 l/4$$

$$dn = \pi \phi l d\phi/2V$$

$$RT \ln p_\phi/p_0 = 2\gamma V/\phi$$

In the above development the length of the cylinder was
taken implicitly as a constant. This will be justified below.

(2) Equivalent Radius of Metal Foil.

Any surface-sensitive thermodynamic function can be used for the development. Pressure is the one most easily visualized.

Assume a disc of radius x and thickness t enclosed in plane surfaces of the same material. At some temperature T the vapor pressure of the surrounding planes is p_o, as is the pressure at the plane faces of the disc. Thus the faces are in equilibrium with the surroundings, and t is invariant. The vapor pressure at the rim is p_t.

As before, $RT \ln p_t/p_o = \gamma \, ds/dn$ (1)

$$s = 2\pi x^2 + 2\pi xt$$ (2)

$$ds = 4\pi xdx + 2\pi tdx$$ (3)

$$n = \pi x^2 t/V$$ (4)

$$dn = 2\pi xtdx/V$$ (5)

Substituting (3) and (5) into (1) and clearing gives

$$RT \ln p_t/p_o = \gamma V(2/t + 1/x)$$

For the case of a very thin disc, (foil), $x \gg t$, and this reduces to $2\gamma V/t$.

Thus, in applying the Kelvin Equation to a cylinder, the diameter ϕ of the cylinder should be used in place of the radius r of the particle. For a plate, the thickness "t" should be substituted.

APPENDIX B   Integration of Equation 15, Page 29

Making the substitution $\ell = x$, to avoid confusion between the letter "ℓ" and the numeral "1", the equation to be solved is

$$dx/dt = wx^2/6\eta V - \ell/6\eta \sqrt{\pi/V} \cdot x^{3/2} \tag{1}$$

Let $a = -\ell/6\eta \sqrt{\pi/V}$, and $b = w/6\eta V$

$$dt = dx/(bx^2 + ax^{3/2}) \tag{2}$$

$$= \frac{1}{x^{3/2}(bx^{\frac{1}{2}} + a)} dx \tag{3}$$

General integration of (3) gives, (Pierce, equations 62 and 65)

$$t = 1/a \int dx/x^{3/2} - b/a \int \frac{dx}{x(bx^{\frac{1}{2}} + a)} \tag{4}$$

$$= \frac{-2x^{-\frac{1}{2}}}{a} - 2b/a^2 \ln x^{\frac{1}{2}}/(bx^{\frac{1}{2}} + a)$$

Taking 0 and t as limits of t, and x_o and x as limits of x gives:

$$t = -\frac{2}{a}(1/\sqrt{x} - 1/\sqrt{x_o}) + 2b/a^2 \ln \frac{x_o(b\sqrt{x} + a)}{x(b\sqrt{x_o} + a)} \tag{5}$$

Substituting for a and b, and noting that $\sqrt{V/\pi} = r_o\sqrt{x_o} = r\sqrt{x}$,

$$t = 12\eta/\ell(-\Delta r + w/\pi\ell \ln \sqrt{x_o/x} \left(\frac{w\sqrt{x} - \ell\sqrt{\pi V}}{w\sqrt{x_o} - \ell\sqrt{\pi V}}\right)) \tag{6}$$

The following substitutions can be made in equation (1)

$$\frac{dx}{dt} = x \frac{d\xi}{dt}, \quad w = \pi r^2 \sigma, \quad V = \pi r^2 x$$

$$\frac{d\mathcal{E}}{dt} = \frac{wx}{6\eta V} - \frac{\gamma}{6\eta}\sqrt{\frac{\pi x}{V}} \tag{1a}$$

$$\frac{d\mathcal{E}}{dt} = \frac{1}{6\eta}\left(\frac{\pi r^2 \sigma x}{\pi r^2 x} - \gamma\sqrt{\frac{\pi x}{\pi r^2 x}}\right) \tag{1b}$$

$$\frac{d\mathcal{E}}{dt} = \frac{1}{6\eta}\left(\sigma - \gamma/r\right) \tag{1c}$$

The same substitutions in equation (6) yield:

$$t = \frac{12\eta}{\gamma}\left[\frac{r_0 \mathcal{E}}{2} + \frac{r_0^2 \sigma}{\gamma}\left(\ln\sqrt{\frac{x_0}{x}}\ \frac{\pi r_0^2 \sigma\sqrt{x} - \pi r\gamma\sqrt{x}}{\pi r_0^2 \sigma\sqrt{x_0} - \pi r_0\gamma\sqrt{x_0}}\right)\right] \tag{6a}$$

Note that $\mathcal{E} = -\frac{2\Delta r}{r_0}$, very nearly. Strictly speaking,

$\Delta r = r_0(1 - \sqrt{1 - \mathcal{E}})$.

Simplifying this as far as possible yields:

$$t = \frac{12 r_0 \eta}{\gamma}\left(\frac{\mathcal{E}}{2} + \frac{r_0 \sigma}{\gamma}\ln\frac{\sigma r_0^2 - \gamma r}{\sigma r_0^2 - \gamma r_0}\right) \tag{6b}$$

This expression still has a variable other than strain, namely "r". However,

$$\mathcal{E} = \frac{4A}{A_0} = \frac{A_0 - A}{A_0} = \frac{r_0^2 - r^2}{r_0^2}$$

Thus $r^2 = r_0^2(1 - \mathcal{E})$ and
$$r = r_0\sqrt{(1 - \mathcal{E})}$$

It is merely a matter of algebraic convenience that equation (1c) is in terms of length and (6b) is in terms of radius. Note also that equation (6b) is an exact expression, despite the fact that σ and $\mathcal{E}$ are ordinary stress and strain.

APPENDIX C   Vapor Pressure of Copper and Dissociation Pressure

of Copper Oxide

Kelley's data on solid copper yields:

$$- \ln P = \frac{41,132}{T} + 0.237 \ln T + 0.000368\ T - 17.82$$

At 1200°K (927°C), $P = 0.83 \times 10^{-8}$ Atm $= 6.3 \times 10^{-6}$ m.m.

At 1350°K $P = 0.37 \times 10^{-6}$ Atm $= 2.8 \times 10^{-4}$ m.m.

The following data are required to calculate dissociation

pressures of the copper oxides.

	Cu		CuO			Cu$_2$O		O$_2$		
	a	b x 10^3	a	b x 10^3	c x 10^{-5}	a	b x 10^3	a	b x 10^3	c x 10^{-5}
Cp	5.44	1.462	10.87	3.576	1.506	13.0	6.0	8.27	0.258	1.877
ΔS^{o}_{298}	7.97		10.4			24.1		49.03		
ΔH^{o}_{298}	0		38.5			42.5		0		

The pertinent equations are:

$$\Delta F = \Delta H^{o}_{0} - \Delta a\ T \ln T - \frac{\Delta b}{2}\ T^2 + \frac{\Delta c}{2}\ T^{-1} + I\ T = -\ RT \ln P \qquad (1)$$

which yields, for $\Delta F = 0$,

$$-\ R \ln P + \Delta a \ln T + \frac{\Delta b}{2}\ T + \frac{\Delta c}{2}\ T^{-2} = \frac{\Delta H^{o}_{0}}{T} + I \qquad (1a)$$

$$\Delta H^{o}_{298} = \Delta H^{o}_{0} + \Delta aT + \frac{\Delta b}{2}\ T^2 + \Delta cT^{-1} \qquad (2)$$

$$\Delta F^{o}_{298} = \Delta H^{o}_{298} - T\ \Delta S^{o}_{298} \qquad (3)$$

The first reaction investigated was:

$$2 \, CuO = Cu_2O + \tfrac{1}{2} \, O_2 \qquad\qquad\qquad (a)$$

For this reaction;

$\Delta H^o_{298} = 34.5 \, K \, cal; \quad \Delta a = -4.6, \, \Delta b = -1.1, \, and \, \Delta c = -2.08$

$$\Delta H^o_o = 34,500 + 4.6(298) + 1.1\frac{(298^2)}{(2000)} + 2.08\left(\frac{100,000}{298}\right)$$

$$= 36,620$$

$\Delta S^o_{298} = 27.8, \, whence \, \Delta F^o_{298} = 26,200$

Inserting these values into the first part of equation (1), at 298°, gives for the integration constant, $I = -60.2$

Thus, omitting some of the arithmetic;

$\log P = 13.16 - 8003 \, T^{-1} - 2.32 \log T - 1.20 \times 10^{-4}T + 22,700T^{-2}$

T^oK	13.16	$-8003T^{-1}$	$-2.32 \log T$	$-1.20 \times 10^{-4}T$	$+ 22,700T^{-2}$	$\log P$	P (atm)
1100	13.16	-7.28	-7.05	-.13	+.02	-1.28	0.052
1200	13.16	-6.70	-7.15	-.14	+.02	-0.81	0.16
1300	13.16	-6.16	-7.23	-.16	+.02	-0.37	0.43

For the second reaction:

$$Cu_2O = 2 \, Cu + \tfrac{1}{2} \, O_2 \qquad\qquad\qquad (b)$$

$\Delta H^o_{298} = 42.5; \, \Delta a = 2.02; \, \Delta b = -2.95; \, \Delta c = -0.939, \, \Delta S^o_{298} = 16.36$

whence $\Delta H^o_o = 41,720$ and $\Delta F^o_{298} = 37,630$

$$I = -4.7$$

The equation for log P then becomes

$$\log P = 1.03 - 9110\ T^{-1} + 1.016 \log T - 6.43 \times 10^{-4}\ T - 10{,}260\ T^{-2}$$

$T(°K)$	1.03	$-\dfrac{9110}{T}$	1.016 $\log T$	$-6.43 \times 10^{-4}\ T$	$-\dfrac{10{,}260}{T^2}$	$\log P$	$P(atm)$	$5P(mm)$
1100	1.03	−8.28	3.09	−0.71	−.01	−4.88	$.132 \times 10^{-4}$	0.050
1200	1.03	−7.59	3.13	−0.77	−.01	−4.21	$.620 \times 10^{-4}$	0.24
1300	1.03	−7.01	3.16	−0.84	−.01	−3.67	2.14×10^{-4}	0.81

The last column represents the maximum air pressure in a kinetic vacuum system, which copper can withstand without oxidizing.

APPENDIX D Vapor Pressure and Solubility of Various Metals

In the following table is given a list of metals having vapor pressures of 10^{-4} atmosphere or higher in the solid state. These metals are worthy of investigation for the determination of surface tension from the vapor pressure of fine wires.

Element	Temperature, $^{\circ}K$ for P = 10^{-4}	Melting Point, $^{\circ}K$	% M.P. to yield 10^{-4} atm.
As	581	Subl	
Ba		1123	
B		2573	
Cd	580	594	97.5
Ca	961	1083	88.8
C	3530	Ca. 3800	93.0
Cr	1693	1888	89.7
Mg	789	924	85.4
Mn	1388	1533	90.6
Sr		1073	
Zn	672	692	97.1

Magnesium, manganese, and chromium appear more favorable than the rest.

If interfacial tension in liquid-solid systems is to be determined from solubility as a function of particle size, the following systems should be considered.

System A – B	Temperature °C	Solubility of solid A in liquid B	Solubility of liquid B in solid A
Cr – Ag	1400	5%	nil
Ni – Ag	1400	4%	3%
Co – Bi	1200	6%	nil
Cu – Bi	700	8%	"
Bi – Ga	200	9%	"
Zn – Bi	400	14%	"
Cd – Ga	200	8%	"
Co – Pb	1300	3%	"
Cu – Pb	900	6%	"
Zn – Pb	400	2%	"
Cu – Tl	900	2%	"
Zn – Tl	400	6%	"

APPENDIX E   The Dimensional Stability of the Wire Specimens

There is probably a tendency for the cross-section of the wires to go out of round at the testing temperature, due to surface migration of atoms. The tendency is to approach a cylinder of minimum surface energy. Due to differences in surface energy with orientation, this cylinder will have, on a macro scale, an elliptical rather than circular cross section. The change in shape cannot be handled analytically, and was too small to detect with the optical equipment used in the experiment.

Another source of dimensional instability is evaporation of the wires. It was shown in section IIIA that, despite the higher vapor pressure of the wires as compared to the plane walls of the cells, interchange with the walls leads to a completely negligible weight loss of the wires. However, the entire interior is losing copper by evaporation through the holes in the lid. This loss can be calculated.

There are seventeen holes, each 0.025 centimeters in diameter by 0.32 centimeter long. The lid of the cell makes nearly a perfect fit, and any loss through the cracks can be neglected, especially as some of the holes are partially blocked by the wire specimens.

The vapor pressure of copper at 1050° Centigrade is about 5×10^{-4} millimeters. This can be taken as the partial pressure of copper vapor inside the cell. Free-molecule flow can be assumed, and the partial pressure of copper outside the cell can be taken as zero, as there is a vanishingly small probability of an escaping molecule ever returning

into the cell. Under these conditions the copper loss in grams per second can be expressed[51] by

$$Q_m = \frac{4\sqrt{2\pi}}{3} \frac{1}{\sqrt{RT}} \frac{a^3}{\ell} (p_1 - p_2)$$

where R is the gas constant per gram of copper vapor. Since the RT factor is a consequence of the mean speed of the molecule, R must be expressed in c.g.s. units. Thus

$$gm \; sec^{-1} = \left(\frac{dyne - cm}{gm}\right)^{-\frac{1}{2}} \frac{cm^3}{cm}(dyne \; cm^{-2})$$

$$= dyne^{\frac{1}{2}} \; gm^{\frac{1}{2}} \; cm^{-\frac{1}{2}}$$

$$mt^{-1} = m^{\frac{1}{2}} \ell^{\frac{1}{2}} \; t^{-1} \; m^{\frac{1}{2}} \ell^{-\frac{1}{2}} = mt^{-1}$$

We are interested in the loss per week for **seventeen** holes, so

$$Q_m = \frac{4\sqrt{2\pi}}{3} \times \frac{1}{\sqrt{1.72 \times 10^8}} (48.8 \times 10^{-6}) (0.5) (6.05 \times 10^5) \cdot (17)$$

$Q_m = 0.020$ gms. of copper per week.

The inside area of the cell is about 70 square centimeters, and copper has a density of 8.93, so the surface will evaporate away at the rate of 4×10^{-5} centimeters of depth per week. This is just outside the limits of accuracy of our instruments. Thus, neither change of shape nor decrease of diameter can be measured. However, we are not justified in using the original diameter of the wires to the degree of accuracy with which it can be measured by its weight.

APPENDIX F   Design of Furnace

I.   Thermal Calculations

    (A)   Radial heat loss

        The insulating value of crumpled aluminum foil only, in the furnace as shown in Figure 5, was calculated by assuming the foil to be equivalent to four equi-spaced concentric cylinders. The furnace tube and shell are concentric with these. The hot portion of the tube was taken as 16 inches, all other cylinders being 21 1/8 inches long.

        The engineering expression for radiation loss in concentric cylinders is[52]

$$q_{ij} = A_i \mathcal{F}_{ij} \sigma (T_i^4 - T_j^4) \tag{1}$$

where q_{ij} is the heat loss in BTU/hour

        A_i = surface area of $i\underline{th}$ cylinder

        σ = Stefan-Boltzmann Constant, in British units

        T_i = temperature of $i\underline{th}$ surface in $^\circ$R.

        $\mathcal{F}_{ij}$ = an emission factor

$$\mathcal{F}_{ij} = \left[\frac{1}{F_{ij}} + \left(\frac{1}{\varepsilon_i} - 1 \right) + \frac{A_i}{A_j} \left(\frac{1}{\varepsilon_j} - 1 \right) \right]^{-1} \tag{2}$$

        ε = emissivity

        F_{ij} is a function of the proportion of radiation emitted by i which is intercepted by j. In this calculation, end losses were neglected, so F_{ij} = 1. Another consequence of this assumption is that q_{ij} = constant. $\hspace{2cm}$ (3)

$\ell_1 = 16''$, $\ell_2 = \ell_3 = \ell_4 = \ell_5 = \ell_6 = 21\ 5/8''$

$d_1 = 4''$, $\quad d_2 = 7\frac{1}{4}''$, $\quad d_3 = 9''$, $\quad d_4 = 10\ 3/4''$, $\quad d_5 = 12\frac{1}{2}''$, $\quad d_6 = 15''$

So:

$A_1 = 201$ sq. in. $A_2 = 364$, $A_3 = 452$, $A_4 = 540$, $A_5 = 628$, $A_6 = 754$

$\mathcal{E}_1 = 1$, $\mathcal{E}_2$ was taken as 0.2, and $\mathcal{E}_3 = \mathcal{E}_4 = \mathcal{E}_5 = 0.1$; $\mathcal{E}_6 = 1$

Substituting these values in Equation (2) gives:

$$\mathcal{F}_{12} = \left[1 + 0 + 0.24(4)\right]^{-1} = 0.5 \qquad A_1\mathcal{F}_{12} = 100$$

$$\mathcal{F}_{23} = \left[1 + 4 + 0.6\,(9)\right]^{-1} = 0.1 \qquad A_2\mathcal{F}_{23} = 36$$

$$\mathcal{F}_{34} = \left[1 + 9 + 0.7\,(9)\right]^{-1} = 0.06 \qquad A_3\mathcal{F}_{34} = 27$$

$$\mathcal{F}_{45} = \left[1 + 9 + 0.75(9)\right]^{-1} = 0.06 \qquad A_4\mathcal{F}_{45} = 32$$

$$\mathcal{F}_{56} = (1 + 9 + 0)^{-1} = 0.1 \qquad A_5\mathcal{F}_{56} = 75$$

Substituting these values in (1) and taking note of (3), gives: (4)

$$100(T_1^4 - T_2^4) = 36(T_2^4 - T_3^4) = 27(T_3^4 - T_4^4) = 32(T_4^4 - T_5^4) = 75(T_5^4 - T_6^4) = K$$

where $K = \dfrac{q}{\sigma \times 10^{12}}$ and T is in 1000° R units

T_1 was taken at 2.5, and T_6 at 0.5. (x 1000° R)

Solving for $T_1^4 - T_2^4$ gives

$$T_1^4 - T_2^4 = \frac{T_1^4 - T_6^4}{100}\left(\frac{1}{100} + \frac{1}{36} + \frac{1}{27} + \frac{1}{32} + \frac{1}{75}\right)^{-1} = 3.28 \qquad (5)$$

$T_2^4 = 35.78$

$T_2 = 2.445 \times 10^3$ °R

The solution of equation (4) may not be immediately obvious to the reader. It is done by taking the concentric shells as equivalent to a series thermal or electrical circuit, but with T^4 rather than

T or E as the driving force. One could go on in a similar manner, solving for T_3, T_4 et cetera, but there is no necessity for this. Because of equation (3),

$$q = (A_1 F_{12}) \sigma (T_1^4 - T_2^4) \qquad (6)$$

$$= 100 \sigma \times 3.28$$

where $\sigma = 12.0$ BTU/hr/in^2/(1000°R)^4

$q = 3900$ BTU/hr $= 1140$ watts

This heat loss was considered too high, and a study of equation (4) will show that the thermal resistivity is very low in the region of the furnace tube, where $T_i^4 - T_j^4$ can have a very high value for a small ΔT. Accordingly, the losses were recalculated on the basis of the substitution of two inches of H-W 20 insulating refractory for the foil next to the tube. It is necessary to calculate this loss by successive approximations. A temperature is assumed for the outer skin of brick, and the heat flow through the brick compared to that through the crumpled foil. A second assumption is then made, in the light of the discrepancy. In this case, the foil was assumed equivalent to three concentric cylinders. T_1 and T_2 are now the inner and outer brick temperatures.

(1) Take $T_2 = 1500°$ R

$\dfrac{T_1 + T_2}{2} = 2000°$ R $= 1560°$ F. At this temperature the thermal conductivity of HW 20 is[53]

$$k = 0.012 \text{ BTU/in}^2/°F/hr/in$$

$$\ell = 2" \qquad A \text{ mean} = 280 \text{ in}^2$$

so $q/\Delta T = \dfrac{kA}{\ell} = 1680$ B/hr/1000° R

$$1680(T_1 - T_2) \overset{?}{=} 36\,\sigma(T_2{}^4 - T_3{}^4) = 27\,\sigma(T_3{}^4 - T_4{}^4) = 32\,\sigma(T_4{}^4 - T_5{}^4)$$

$$= 75\,\sigma(T_5{}^4 - T_6{}^4) = q^1$$

where the areas and emission factors are taken from the previous calculation.

$$T_2{}^4 = 5.06, \qquad T_6{}^4 = 0.06,$$

so, in analogy to equation (5);

$$T_2{}^4 - T_3{}^4 = \frac{5}{36\sigma}\left(\frac{1}{36} + \frac{1}{27} + \frac{1}{32} + \frac{1}{75}\right)^{-1} x\,\sigma = \frac{5}{36}\frac{(1)}{(.109)} = 1.275$$

This yields a heat flow through the foil of

$$q^1 = 36 \times 12 \times 1.275 = 550 \text{ B/hr}$$

indicating that the first guess as to the insulating value of the brick was too optimistic. Inspection showed that $T_2{}^4$ should be about 10 (again in 1000° R units), so T_2 was taken at 1800° R

$$T_2{}^4 = 10.50$$

$$q = 1680\Delta T = 1175 \text{ BTU/hr}$$

$$T_2{}^4 - T_3{}^4 = \frac{10.46(1)}{36\,(.109)} = 2.66$$

$$q^1 = 36 \times 12 \times 2.66 = 1150 \text{ B/hr}$$

This check, 1175 versus 1150, was considered satisfactory, and 1150 B/hr, equal to 340 watts, was taken as the value for radial heat loss.

(B) Axial heat losses

(1) Radiation

This loss is of the form

$$q = \sigma \int_o^4 \phi(x)\,(T_1{}^4 - T_x{}^4)\,dx$$

where $\phi(x)dx$ is a differential function which would integrate to an $\mathcal{F}_{ij}$ value, and T_x is a function of x. If $\mathcal{E}(T)$ and $k(T)$ for Inconel are known, this integral can probably be evaluated by the calculus of variations, but the labor would be prohibitive. Accordingly, it was assumed that T_x is linear and the radiation is all concentrated in a conical beam emitted normal to the median circle of a hemisphere. This hemisphere is one half of the spherical black body equivalent of the hot tube. Figure 21 is a graphical representation of this approximation. (The assumption is completely intuitive.)

$$q = \frac{2 \times 2\pi}{144} \times 1730(39.06 - 19.45) = 2960 \text{ B/hr} = 860 \text{ watts}$$

(2) Conductive:

$$q = \frac{kA}{\ell}(T_1 - T_2)$$

For Inconel, $k = 104$ B/hr/ft^2/$^\circ$F/in

$$= 0.72 \text{ B/hr/in}^2/^\circ\text{F/in}$$

$$\ell = 4"$$

$$A = \frac{\pi}{4}(6.25 - 4.00) = 1.76 \text{ in}^2$$

$$T_1 = 2050 \ ^\circ\text{F}, \ T_2 = 150 ^\circ\text{F}$$

$$q = 0.72 \ \frac{1.76}{4} \times 1900 = 602 \text{ B/hr} = 176 \text{ watts}$$

This is the loss at each end, so the two ends lose 350 watts by conduction. The total of the three items is 1550 watts.

(C) Winding Calculations

To obtain control over uniformity of temperature distribution at least three independently controlled circuits are desirable. Parallel windings with series rheostats are the most convenient, although the same control can be achieved with series windings and shunt

Figure 21: GRAPHICAL APPROXIMATION FOR RADIATIVE HEAT LOSS

Figure 22: GRAPHICAL SOLUTION OF FURNACE WINDING TAPER

500°R   2100° 2500°R

$A_1 = A_2$

END CONDUCTION

AXIAL RADIATION

RADIAL RADIATION

WATTS REQUIRED PER INCH OF TUBE

200

100

6   5   4   3   2   1   0
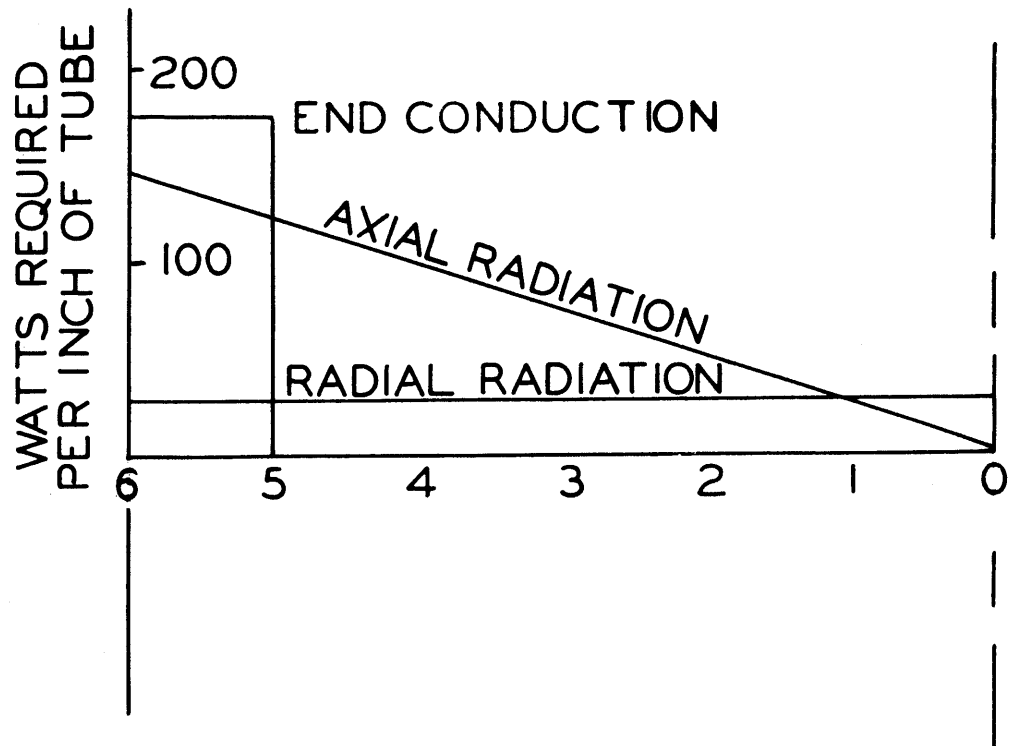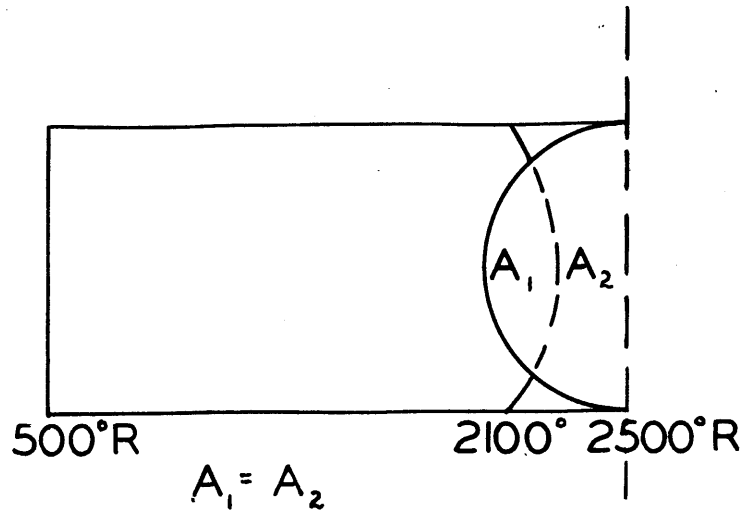
rheostats. Operation at 115 Volts or 230 Volts was considered most favorable, although a step-down transformer can often be used to advantage on a small furnace.

From the fundamental expressions:

$$P = V^2/R \qquad (1)$$

$$R = \rho \ell/A = \frac{4\rho\ell}{\pi d^2} \qquad (2)$$

$$S = \pi d \ell \qquad (3)$$

it can readily be derived that

$$d = \frac{1}{335.3} \sqrt[3]{\left(\frac{P}{V}\right)^2 \frac{\rho}{p}} \qquad (4)$$

Where P = power input to a winding element in watts

   V = applied E.M.F.

   R = resistance of element

   ρ = resistivity of element alloy in ohms per circular mil foot.

   ℓ = developed length of element

   d = diameter of element wire in inches

   S = surface area of element in square inches

   p = surface loading of element in watts per square inch.

P = 600 watts per element

p = 10 watts per square inch

ρ = 697 Ω/cmf for Tophet A at 1000°C

Substituting these values into equation (4) gives a diameter of .037 inch at 115 volts.

The nearest commercial wire size to this is 19 gauge. The winding resistance, regardless of size, must be $V^2/P = 22.0$ ohms. Nineteen gauge Tophet A has a resistance of 0.537 ~/ft at $1000°C$, so a length of 41.0 feet would be required. For this,

$$s = \pi d \ell = 55.7 \text{ sq. in.}$$

$$p = P/s = 12.5 \text{ watts/in}^2$$

Thus 18 gauge wire is required.

$$R = 0.435 \text{ ~/ft.}$$

$$\ell = 50.5 \text{ ft.}$$

$$s = 76.2 \text{ sq. in.}$$

$$p = 9.2 \text{ watts/sq.in.}$$

It is evident without calculation that at 230 volts the wire would be much too long and fine to construct a rugged winding. Similar calculations for series elements led to 38 feet of 16 gauge wire at 230 volts and 23 feet of 12 gauge wire at 115 volts. The latter would be awkward for use on a tube furnace of the dimensions required; too short and stiff for coiling, but too long to apply uncoiled. Series elements at 230 volts would be somewhat more rugged than parallel elements at 115 volts, but not enough so to justify the inconvenience of shunt controls. Accordingly, it was decided to use the 18 gauge wire.

The element distribution was calculated graphically. Figure 22 shows the method used. In this diagram the abscissa is length from the center of the furnace tube, and the ordinate is heat loss per unit length. Each of the areas (two rectangles and a triangle) represents

a component of loss in watts. It is evident that for perfect
uniformity along the heated length, the two end coils of wire would
have to supply all the axial conduction loss, which is impossible.
Accordingly it was assumed that a gradient exists in the last inch
of the hot zone sufficient to supply the driving force for this loss.
This is represented by the tall rectangle at the left end of the
diagram. This gradient is ignored when assuming that radial heat
loss is uniform and confined to the heated zone. Axial radiation
was assumed to be a linear function of distance from the origin.
The power requirements for each inch of length can now be read
directly from the diagram.

A reader who is unfamiliar with thermal calculations may be
confused by the use of the watt as a unit of heat loss. The unit is
energy per unit time, say BTU/hr. B.T.U's are converted to electrical
energy units, watt hours for example, and watt hours of energy per
hour are obviously equivalent to watts of power.

The only obtainable grooved alundum tube of the dimensions re-
quired was one with a pitch of six per inch. The use of alternate
grooves gave three turns of coil per inch. The tube has an outside
diameter of 3 inches, so the mean coil diameter is about $3\frac{1}{4}$ inches.
Thus there is $3 \times 3\frac{1}{4}\pi = 30.7$ in. of coil per inch of tube. Eighteen
gauge wire wound around on a 3/16 inch mandrel has a coil width of
0.278 inch, so the spacing between coils at their closest approach
is 0.055 inch. The close wound length per element (50.5 ft.) is
34 inches or 17.65 watts per inch, so $17\frac{1}{2}$ inches of close wound element

is required to just balance the heat loss of the first inch of tube. (Table III) For a coil length of 30.7 inches per inch of tube, this portion of the element must be stretched to 1.75 times its close wound length. In a similar manner the required close-wound length for each inch is calculated. Rows e and f of Table III show the results of this calculation. As each element is 34 inches long (close wound) there is a full element on 2 2/3 inches at each end, and the third element is spread over 6 2/3 inches in the middle.

TABLE III

Distance to furnace center in inches.		6-5	5-4	4-3	3-2	2-1	1-0
(a)	Axial conduction loss (watts)	176	0	0	0	0	0
(b)	Axial radiation loss (watts)	132	108	84	60	36	12
(c)	Radial losses (watts)	28	28	28	28	28	28
(d)	Surplus (1)	0	42	21	21	21	21
	Total	336	178	133	109	85	61
(e)	C.W. inches required	$17\frac{1}{2}$	$11\frac{1}{2}$	$7\frac{1}{2}$	$6\frac{1}{4}$	4 3/4	$3\frac{1}{2}$
(f)	L/L_{CW} (2)	1.75	2.67	4.10	4.91	6.46	8.77

(1) As the losses total up to less than the winding capacity, there is surplus winding to be distributed. There was no room for any of this surplus in the end turns.

(2) L = the actual length of three turns, = 30.7 inches.

C.W. = close-wound.

It may be of interest to compare the actual with the predicted performance of the furnace. As already mentioned, the total heat loss checked the calculated figure very closely. It was always possible to adjust the winding currents so that a 5 inch zone was uniform to $\pm$ 1 or 2 degrees. However, the rough estimate on distribution of losses was considerably in error. Thus at $1000^{\circ}C$ the end windings required about twice as much power each than the center winding. This is quite reasonable if the ends of the hot zone supply the bulk of the axial radiation loss.

II. Temperature and Vacuum Control

(A). Power Circuit

A Tagliabue Celectray proportioning controller was used for automatic temperature control. In this instrument, a light beam is directed from a galvanometer mirror to a photoronic cell. A motor-driven "throttling edge" periodically interrupts this beam, disconnecting the furnace from the mains. The optical system is so arranged that the duration of the off period is directly proportional to the difference between furnace temperature and controller setting. A throttling range of $60^{\circ}C$ is used; i.e. at more than 30° below controller setting the furnace is on 100 per cent of the time, and at 30° above it is off 100 per cent of the time. With a one minute off-on cycle, no fluctuation in the temperature was detectible on a recorder chart readable to $\pm \frac{1}{2}^{\circ}C$.

The Tag instrument is not self-balancing, nor does it have automatic droop compensation. The former defect does not introduce a measurable drift in ten hours, the longest period over which the

equipment ran unattended. However, Building 35 does suffer a diurnal voltage variation which introduces a drift of $\pm$ 3°C during long unattended periods.

Five thermocouples were used. A 20-gauge Chromel-Alumel couple at the center of the furnace was connected to the controller. A platinum-platinum 10 per cent Rhodium couple extended 3/4 inch further, and was inserted into a molybdenum-lined copper thermocouple well in the specimen holder. A 24-gauge chromel-alumel couple had its junction close to the controller couple, and two similar chromel-alumel couples were placed $2\frac{1}{2}$ inches ahead and behind. These latter four couples were connected through an ice junction to a Leeds and Northrup double-range portable potentiometer, Serial Number 73113.

The precious metal couple was used as the standard, and the controller was merely set to whatever point gave the desired temperature in the specimen holder. The control rheostats (A, figure 23) were adjusted to bring the other three couples to within 2 or 3°C of each other. As the specimen holder is of massive copper and is only $1\frac{1}{4}$ inches long, its inside temperature was undoubtedly uniform to $\pm \frac{1}{2}$°C or less.

The Powerstat variable transformer shown in Figure 23 was practically superfluous. It was used only in baking out the furnace. It will be required, however, if the unit is used for lower temperature work.

(B). Vacuum Assembly

As previously mentioned, the vacuum system was tremendously overdesigned, so that the unit could be used for vacuum sintering. A Distillation Products Company Type MC-275 metal diffusion pump was used, backed up with a Kinney pump, Type VSD, Size 556. Amoil-S was used as

Figure 23:   CIRCUIT DIAGRAM OF THE APPARATUS
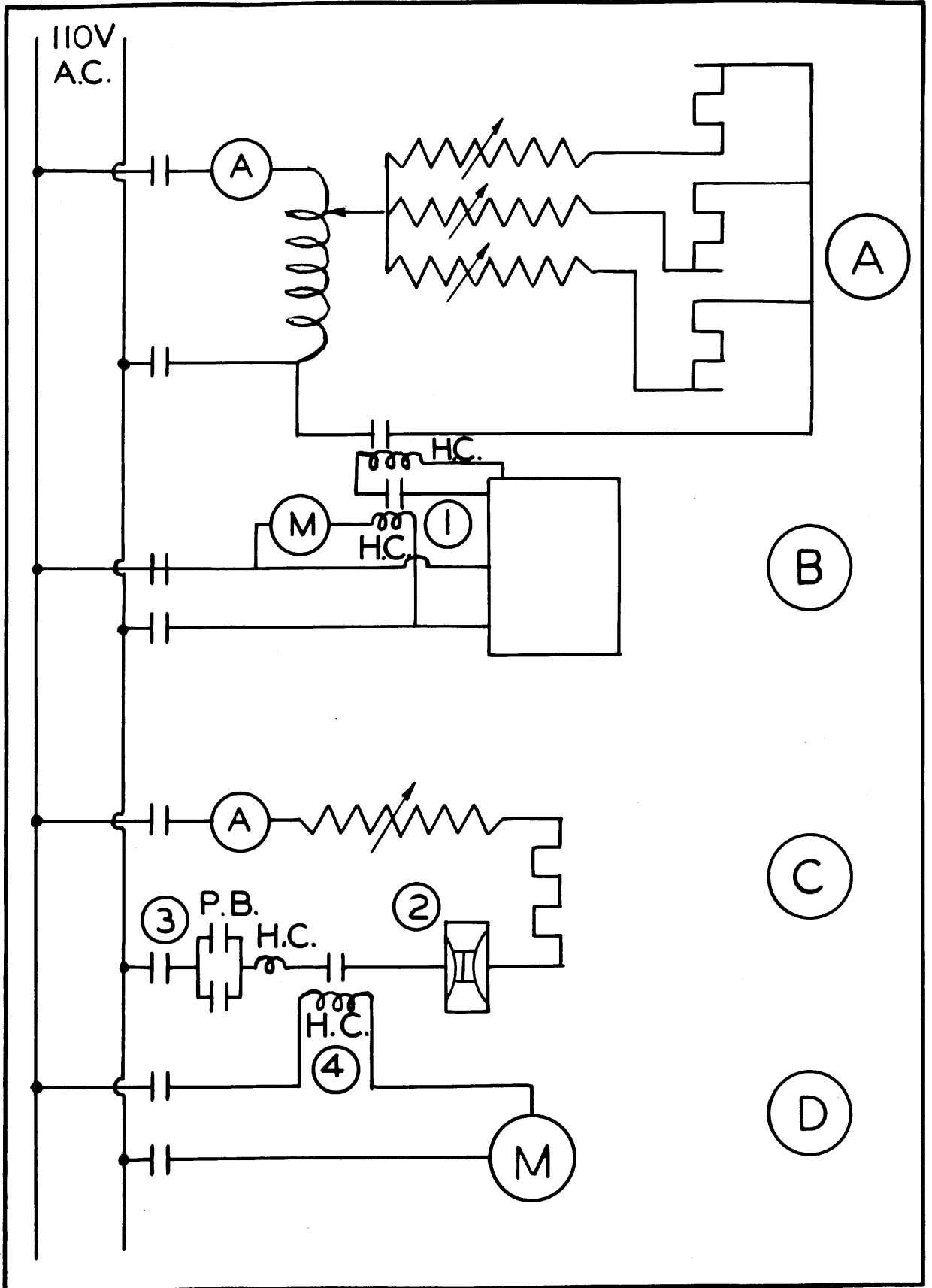
        A - Furnace Section

        B - Controller Section

        C - Diffusion Pump

        D - Roughing Pump

        See text for significance of (1), (2), (3), and (4)

110V
A.C.

H.C.

M
H.C.

I

A

B

A

P.B.
3
H.C.
2

C

H.C.
4

M

D

a diffusion pump fluid. The Kinney was itself capable of holding the system at 0.03 millimeter pressure, and is rated at 8 C.F.M. capacity at 450 R.P.M. and 0.1 millimeter pressure. The MC 275 pump is rated at 275 liters per second at 2×10^{-4} millimeters,(P_1) and at 3.25 amperes heater current has a capacity of 175 L.P.S at 10^{-5} millimeters when working into 0.1 millimeter fore pressure.(P_2) 8 CFM is 3.8 L.P.S. and 275 (P_1/P_2) is 0.55 L.P.S., so the Kinney pump can handle any surges of gas the diffusion pump may deliver.

If the gas source is taken at the center of the hot zone the connecting system consists of 18 inches of furnace tube at 2 inches diameter, and 18 inches of connecting pipe at $2\frac{1}{4}$ inches diameter. The gas in the former is at a mean temperature of about 900° K and in the latter is at about 400°K. This system will have a resistance to free molecule air flow of[54]

$$W = 1.59 \times 10^{-5} \left[\sqrt{\frac{273 \times 29}{900}} \left(\frac{18 \times 2.54}{(2 \times 2.54)^3} \right) + \sqrt{\frac{273 \times 29}{400}} \left(\frac{18 \times 2.54}{(2\frac{1}{4} \times 2.54)^3} \right) \right]$$

$$W = 3.40 \times 10^{-5} \text{ sec/cc}$$

so the system capacity is about 30 L.P.S. Thus an outgassing volume of 0.03 cc/sec S.T.P. can be handled at a furnace pressure of 10^{-3} millimeters.

(C). Protective Devices

The interlocking relay system shown in the circuit diagram, Figure 23, is on hand, but has not yet been installed in the apparatus. Number 1 is an auxiliary relay with its coil in series with the throttling

motor of the controller and its contact in the furnace relay circuit.
If the throttling motor should fail when the photronic relay is in
the on position, the furnace temperature would rise to dangerously
high levels. The auxiliary relay automatically disconnects the
furnace in case of such a failure.

Number 2 is a Fenwal Thermoswitch at the efflux end of the
diffusion pump cooling coil. It is set to open at 170°F. If the
cooling water supply should fail this switch will disconnect the
diffusion pump heater from the power mains. Number 3 is merely a
holding relay to prevent the pump from coming back on the line when
its stagnant water cools below 170°.

Number 4 is a relay with its coil in series with the Kinney
pump motor and its contacts in the diffusion pump heater line. Thus
failure of the Kinney pump will cause the diffusion pump to drop off
the power mains. The entire cost of this interlocking system is less
than the replacement cost of one batch of pump fluid.

APPENDIX G   Description of Preliminary Experiments

In Test Number 1 we were looking for the order of magnitude of the surface tension effect. Six weighted wires were hung from an open nichrome frame, and were measured from the suspension point to the weight, to the nearest 1/64th inch. In 24 hours at 1025°, these specimens lost one half their original diameter.

Test Numbers 2 to 5 were conducted in a copper cell, with chrome-plate to delineate the gauge lengths. The specimens were measured in tension in a horizontal jig. De-mounting and jigging the specimens after test led to plastic deformation, and the results were worthless.

Tests Numbers 6 and 7 were similar. The specimens were measured in situ, but without special precautions against damage. Subsequent to these tests, a vapor-deposited film of chromium was found on the cell walls. Chrome plating was thus indicated as a source of surface contamination.

Test Number 8 was run like the subsequent ones discussed in the body of this thesis, except that no preliminary anneal was used. Two of the six specimens were damaged before a technique of measuring the specimens without ever touching them was developed.

APPENDIX H   Typical Calculations

I.   A typical Stress-Strain Determination on Double-Knotted Wires

   This is for Test Number 13.   Eight 0.005 inch specimens were annealed for $1\frac{1}{2}$ hours at 1050°, and heated for $24\frac{1}{4}$ hours at 1050°.

Specimen Number	Initial Lengths (cm) Knot-to-knot	Knot-to Wgt	Final Lengths (cm) K - K	K - W	$\underline{Wo}$(Mg)	$\frac{1}{2}W_\ell$
1	2.124	2.292	2.115	2.281	0	1.2
2	1.845	2.185	1.838	2.179	10.2	1.1
3	1.504	1.858	1.500	1.854	16.4	0.9
4	1.866	2.103	1.864	2.103	29.4	1.1
5	1.781	2.066	1.783	2.069	36.6	1.0
6	1.841	2.013	1.845	2.018	36.2	1.1
7	1.619	1.821	1.626	1.827	45.3	0.9
8	1.844	2.018	1.854	2.029	58.5	1.1

Specimen Number	W	σ (dynes/cm^2 x 10^{-4})	ε, cm/cm x 10^3	$\varepsilon_{_\curlywedge}$	$\varepsilon_{av.}$
1	1.2	.91 x 10^4	-4.2	-4.8	-4.5
2	11.3	8.61	-3.8	-2.8	-3.3
3	17.3	13.19	-2.8	-2.2	-2.5
4	30.5	23.15	-1.1	0	-0.5
5	37.6	28.65	+1.1	1.5	+1.3
6	37.3	28.42	2.2	2.5	+2.4
7	46.2	35.2	4.3	3.3	3.8
8	59.6	45.45	5.4	5.4	5.4

II. A typical time-temperature-vacuum log.

This is for Test Number 14. 0.003 inch specimens at 1050°.

Date	Time	Controller Setting (°F)	Controller Reading	West C-A Couple (MV)	Center Couple °F
9/30/48	1440				
	1540	1936	1936	43.65	1951
	1700	1935	1935	43.7	1951
	2300	1935	1937	43.7	1954
10/1/48	900	1937	1937	43.85	1960
	1400	1937	1937	43.70	1955
	1700	1937	1936	43.75	1958
10/2/48	900	1937	1937	43.7	1958
	1200	1938	1938	43.7	1958
	1340				

Date	Time	East Couple (MV)	Mean of East and West Couples, °F	Plat. - Rhod. Couple MV.	°C
9/30/48	1140			10.15	1050
	1540	43.75	1944	10.16	1051
	1700	43.7	1944	10.15	1050
	2300	43.7	1944	10.15	1050
10/1/48	900	43.75	1949	10.19	1054
	1400	43.70	1949	10.15	1050
	1700	43.70	1950	10.16	1051
10/2/48	900	43.7	1950	10.15	1050
	1200	43.7	1950	10.16	1051
	1340			10.15	1050

Throughout this test, the Thermocouple Vacuum Detector read 192 microamperes, equivalent to about 3×10^{-5} millimeters of mercury. In this test the center chromel-alumel couple was connected to a Leeds and Northrup strip-chart potentiometer recorder instead of to the potentiometer indicator. It had been previously determined that the former reads $8°F$ higher than the latter, probably due to imperfect cold-junction compensation in the recorder.

III. A typical Least Square Solution of Stress-Strain-Data

From the equation

$$\varepsilon = a + b\sigma \tag{1}$$

where $a = -t\gamma/6\eta r$ and $b = t/6\eta$

the normal equations

$$\sum \varepsilon - na - b\sum\sigma = 0 \tag{2}$$

$$\sum \varepsilon\sigma - a\sum\sigma - b\sum\sigma^2 = 0 \tag{3}$$

where n = number of observations

are obtained.[43] These equations are solved simultaneously for a and b.

It is evident from equation (1) that for $\varepsilon = 0$, $\sigma = -\frac{a}{b} (= \sigma_y)$. It will be recalled that $\gamma = \sigma_y r$. Also, from equation (1), $\eta = t/6b$

$\varepsilon \times 10^4$	$\sigma \times 10^{-5}$	$\varepsilon \times \sigma \times 10^{-1}$	$\sigma^2 \times 10^{-10}$
-107	.072	-7.70	.005
- 57	1.179	-67.20	1.390
- 21	2.455	-51.55	6.027
- 9	3.393	-30.54	11.512
- 6	3.635	-21.81	13.213
+ 2	4.235	+ 8.47	17.935
+ 46	5.540	+254.84	30.692
+ 91	8.135	740.29	66.178
+139	28.64	+1003.60	146.95
-200		- 178.80	
- 61		+ 824.80	

$- 61 - 8a - 28.64b = 0$

$+ 824.8 - 28.64a - 146.95b = 0$

$- 218.5 - 28.64a - 102.53b = 0$

$$44.42b = 1043.3$$

$$b = 23.5 \ (\times 10^{-9})$$

$8a = -61 - 674 = -735$

$a = -91.9 \ (\times 10^{-4})$

$\sigma_\gamma = 3.91 \times 10^5 \ \text{dynes/cm}^2$

$\gamma = 1410 \ \text{dynes/cm}$

$t = 72 \ 1/3 \ \text{hours} = 2.604 \times 10^5 \ \text{sec}$

$\eta = \dfrac{2.604 \times 10^5}{6 \times 23.5 \times 10^{-9}} = 1.847 \times 10^{12}$

Bibliography

(1) Becker,   Ann. Phys. $\underline{32}$, 128 (1938)

(2) Smith,   Met. Tech. T.P. 2387, June, 1948

(3) Rhines,   T.A.I.M.E. $\underline{166}$, 474 (1946)

(4) Gibbs,   Collected Works, Vol. I, P. 219 ff
             N. Y. Longmans, Green, 1931

(5) Gibbs,   Loq. Cit. p. 229

(6) Saal and Blott,   Physica $\underline{3}$, 1099 (1936)

(7) W. Ostwald,   Z. Physik. Chem $\underline{34}$, 503. (1900)

(8) Pawlow,   A. Physik. Chem. $\underline{65}$, 1 (1909)

(9) Kossel,   Ann Phys.(5) $\underline{21}$, 457 (1934)

(10) Jones, W.D.   Metal Treatment $\underline{13}$, 265 (Winter 1946-47)

(11) Fricke and Meyer,   Z. Phys. Chem. $\underline{A181}$, 409 (1938)

(12) Lipsett, Johnson, and Maass,   J.A.C.S. $\underline{49}$, 925, 1940 (1927)

(13) Meissner,   Z. Anorg. allgem. Chem $\underline{110}$, 169 (1920)

(14) Skapski,   Private Communication

(15) Turner,   Proc. Roy. Soc. $\underline{A81}$, 301 (1908)

(16) Harkins,   J. Chem. Phys $\underline{10}$, 268 (1942)

(17) Kelley, U.S.B.M. Bulletin $\underline{383}$ (1935)

(18) Pauling,   The Nature of the Chemical Bond, 2nd Ed. p. 409,
             Ithaca, N. Y. - Cornell Univ. Press

(19) Frenkel, J.   J. Chem. Phys $\underline{7}$, 538 (1939)

(20) Turnbull,   M.I.T. Metallurgy Colloquium, Dec. 1, 1948.
             (Unpublished Work)

(21) Hollomon, W.H.   Private Communication

(22) Frenkel, J.   Phil. Mag. 33, 297 (1917)

(23) Dorfman,   C.R. Acad. Sci. URSS 41, 372 (1943)

(24) Brager and Schuchowitzky,   Acta Phys. Chem. 21, 13 (1946)

(25) Turner,   Proc. Roy. Soc. A81, 301 (1908)

(26) Chapman and Porter   ibid. A83, 65, (1909)

(27) Sawai and Nishida   Z. Anorg. allgem. Chem 190, 375 (1930)

                                           193, 1119 (1930)

(28) Tammann   Ann. Phys 12, 820 (1932)

(29) Shaler   Dissertation, M.I.T., Dept. of Met. 1947

(30) Burwell, J.T.   Private Communication

(31) Harkins and Livingston   J. Chem. Phys 10 342 (1946)

(32) Frenkel, J.   USSR J. phys IX, 385 (1945)

(33) Gensamer   Strength of Metals under Combined Stresses, p. 44,
     A.S.M. Cleveland.

(34) Shaler and Wulff   Ind. Eng. Chem 40, 838 (May, 1948)

(35) Gibbs   Loq. Cit. p. 244 f.f.

(36) Paschkis   Industrial Heating 13, 1972 (1946)

(37) Kauzmann   Tran. AIME 143, 67, (1941)

(38) Steigman, Shockley, and Nix   Phys. Rev. 56, 13 (1939)

(39) Benedicks   Pittsburg International Conference on Surface
     Reactions. p. 196 Corrosion Publishing Co.,
     Pittsburg (1948)

(40) Benedicks and Ruben   Jern. Ann. 129, 37 (1945)
                           (As quoted by Benedicks in Ref. 39)

(41) Millard   Physical Chemistry for Colleges, 3rd Ed. p. 80
     N.Y. McGraw-Hill, 1931.

(42) Goodwin   Precision of Measurements and Graphical Methods.
     N.Y. McGraw-Hill, 1920. p. 21

(43) ibid. pp. 64-66

(44) Quincke   Pogg. Ann. 134, 357 (1868)

(45) Libman,   Phys. Rev. 29, 911 (1927)

(46) Sauerwald and Drath   Zeitsch. anorg. Chem. 162, 301 (1927)

(48) Getman and Daniels,   Outlines of Theoretical Chemistry, 6th Ed.
                             p. 219 f. N.Y. Wiley, 1937

(49) Kuczynski,   Bull. Am. Phys. Soc. 23, No. 7, 25 (Nov., 1948)

(50) Kuczynski,   Dissertation. M.I.T., Dept. of Met. 1947

(51) Kinnard,   Kinetic Theory of Gases, 1st Ed. p. 304
                 N. Y. McGraw-Hill, 1938.

(52) Perry,   Chemical Engineers Handbook 1934 ed. p. 885
               N.Y. McGraw-Hill

(53) The Harbison - Walker Company   Private Communication

(54) Strong,   Procedures in Experimental Physics p. 99
                N.Y. Prentice-Hall, 1943

(55) Beck et al   Met. Tech. T.P. 2280 Sept. 1947

Biographical Note

The writer, Harry Udin, was born in Boston, Massachusetts, in 1916. He attended the public schools of Newton, Mass., and matriculated at the Massachusetts Institute of Technology in 1933, where he majored in Electrochemical Engineering, receiving the S.B. degree in 1937. He received a Sigma Xi award on the basis of his undergraduate thesis, on tin extraction from low-grade ores.

From 1937 to 1945 he was employed in the metallurgical laboratories of the United States Metals Refining Company, and from 1945 to 1947 was engaged in similar process research and development with the Reynolds Metals Company. He joined the staff of the Division of Industrial Cooperation at M.I.T. in the spring of 1947, and in the fall of that year was awarded the Revere Fellowship, enabling him to resume his studies. At present he resides, with his wife and two children, in Newtonville, Mass.

ABSTRACT

A knowledge of the surface tension of solid metals is useful in a number of metallurgical problems, and is essential to the study of sintering. A survey of the literature indicated that no reliable method existed for its measurement.

A new experimental method is described in this report which consists of measuring the longitudinal strain in fine wires as a function of load, at elevated temperatures. Both negative and positive strains are found, and the load required to just balance the contractile stress of surface tension is a measure of surface tension. The experiments, conducted on 36 gauge and 40 gauge copper, yielded a value for surface tension of

$$\gamma = 2000 - 0.46\ T$$

where γ = surface tension and T is in $^\circ$K.
The equation is valid to $\pm$ 100 dynes/cm between 950 and 1050°C.

From the magnitude of the strains as a function of stress, time, and temperature, the viscosity of solid copper in the same temperature range can be expressed by

$$\eta = 130 e^{59,000/RT}$$